

## ABSTRACT

LOSSING, JENNIFER AIMEE. Quantification of Chondrocyte Death and Proteoglycan Content in Mechanically Impacted Articular Cartilage. (Under the direction of Peter L. Mente)

Impact injuries can lead to cellular and matrix changes in articular cartilage, similar to those occurring in the pathogenesis of secondary osteoarthritis. The purpose of this study was to examine the changes in cartilage following an impact injury as a model for early osteoarthritic degradation. Using an *in vitro* organ culture model, the proteoglycan content and the viability of chondrocytes relative to the magnitude of an impact injury, the time following the injury and the relative location within the cartilage layer was examined. In this study, it was hypothesized that injurious mechanical loading would result in increased chondrocyte death and decreased proteoglycan content with increasing load and time in culture. Paired porcine knee joints were obtained fresh and patellae were removed using sterile techniques. A total of 36 patellae were used. Twelve patellar cartilage specimens were subjected to controlled mechanical injuries to a force level of 1000 N (medium) and 12 specimens at a force level of 2000 N (high). Twelve patellae were used as non-injured controls. Following impaction, the intact patellae were placed in organ culture for 0, 3, 7 or 14 days and subsequent degenerative changes over time were assessed. Cell viability was quantified using a MTT (3-(4,5-dimethylthiazoyl-2-yl) 2,5-diphenyl-tetrazolium bromide) assay and the percentage of dead cells at various positions was determined. Proteoglycan concentration was measured using Safranin-O staining intensities. There was a significant, location dependent, cell death increase with increasing impact load. A significant location dependent decrease in proteoglycan content was observed from medium impactions, while an increase in proteoglycan content was seen from high impactions. In conclusion, the

magnitude of an impact load can significantly affect the degree of matrix changes throughout the depth of articular cartilage tissue over time.

**QUANTIFICATION OF CHONDROCYTE DEATH  
AND PROTEOGLYCAN CONTENT IN  
MECHANICALLY IMPACTED ARTICULAR CARTILAGE**

By

**JENNIFER AIMEE LOSSING**

A thesis submitted to the Graduate Faculty of  
North Carolina State University  
in partial fulfillment of the  
requirements for the Degree of  
Master of Science

**BIOLOGICAL AND AGRICULTURAL ENGINEERING**

Raleigh

2004

APPROVED BY:

---

**C. FRANK ABRAMS, Jr.**  
Committee Member

---

**SIMON C. ROE**  
Committee Member

---

**GARY A. MIRKA**  
Committee Member

---

**PETER L. MENTE**  
Chair of Advisory Committee

## **Biography**

Jennifer A. Lossing was born on July 25, 1977 in Mississauga, Ontario, Canada. She moved to North Carolina in 1997 and attended The University of North Carolina at Charlotte where she received a Bachelor of Science degree in Biology, with a minor in Anthropology in 2000. A year later, she was accepted into the Graduate School at North Carolina State University where she earned a Master of Science degree in Biological Engineering with a graduate minor in Industrial Engineering in 2004. She is currently a Risk Control and Ergonomic Consultant for Marsh USA Inc.

## **Acknowledgements**

Many thanks to the Tissue Mechanics Lab staff in the Department of Biomedical Engineering for their collaboration and assistance in all experimental procedures. Thank you also to Dr. Peter Mente for his advice and support throughout my academic endeavors. This research was funded by a Whitaker Foundation Biomedical Engineering Research Grant.

## TABLE OF CONTENTS

	Page
LIST OF TABLES.....	vi
LIST OF FIGURES.....	vii
1. Introduction.....	1
2. Cartilage .....	2
3. Articular Cartilage.....	2
3.1 Joint Tissue Structure and Composition.....	3
3.2 Matrix Components.....	4
3.3 Proteoglycans.....	5
3.4 Type II Collagen.....	7
3.5 Chondrocytes.....	9
4. Osteoarthritis.....	11
4.1 Proteoglycan Content and Osteoarthritis.....	12
4.2 Chondrocyte Death and Osteoarthritis.....	12
4.3 Apoptosis and Necrosis.....	13
5. Models of Cartilage Degeneration.....	15
5.1 Techniques for Experimental Loading of Cartilage.....	15
5.2 <i>In vitro</i> Impact Models of Articular Cartilage: Literature Review.....	16
6. Purpose of Study.....	22
6.1 Hypotheses.....	23
7. Methods.....	24
7.1 Randomization of Specimens.....	24
7.2 Porcine Patella Removal.....	26
7.3 <i>In vitro</i> Impactions.....	28
7.4 Organ Culture.....	32
7.5 Tissue Analysis.....	33
7.6 Data Collection.....	35
7.7 Measurement of Safranin-O Staining Intensity: Proteoglycan Content.....	39
7.8 Quantification of Chondrocyte Viability.....	40
7.9 Statistical Analysis.....	41
8. Results.....	42
8.1 Chondrocyte Viability.....	42
8.2 Proteoglycan Content.....	47
9. Discussion.....	52
10. Recommendation for Future Research.....	59
10.1 Stain for General Cell Death, Apoptotic Cell Death and Cell Proliferation.....	59
10.2 Damaged Type II Collagen Analysis.....	59
10.3 Assessment of Tissue Fibrillation and Subchondral Bone Damage.....	60
10.4 Effect of Axial Load on Chondrocyte Shape and Volume.....	60
11. References.....	62

## APPENDICES

A. Porcine Patella Removal.....	68
B. <i>In vitro</i> Articular Cartilage Impaction.....	69
C. Patella Incubation: <i>In vitro</i> Organ Culture.....	70
D. Histology.....	71
D.1 Cell Viability Stain.....	71
D.2 Tissue Freezing.....	73
E. Cell Viability Data.....	75
F. Normalized Intensity Data: Proteoglycan Concentration.....	81

## LIST OF TABLES

Table 1. Randomization of Specimens.....	25
Table 2. Impaction Groupings.....	25
Table 3. Schedule of Experiment Dates and Associated Specimens.....	26
Table 4. Distances From Impaction Center.....	36
Table 5. Data: Percentage of Dead Cells by Tissue Depth.....	75
Table 6. Data: Percentage of Dead Cells by Radial Position.....	78
Table 7. Data: Normalized Intensity by Tissue Depth.....	81
Table 8. Data: Normalized Intensity by Radial Position.....	84



## LIST OF FIGURES

Figure 1. The Knee Joint.....	2
Figure 2. A Porcine Patella.....	3
Figure 3. The Zones of Articular Cartilage.....	4
Figure 4. A Proteoglycan Molecule.....	6
Figure 5. Synthesis, Secretion and Assembly of a Collagen Fiber.....	8
Figure 6. An Articular Cartilage Chondron.....	10
Figure 7. Osteoarthritic Cartilage.....	11
Figure 8. Articular Cartilage Chondrocytes.....	14
Figure 9. Patella in PMMA Mold.....	28
Figure 10. Piezoelectric Load Cell.....	29
Figure 11. The MTS Mini Bionix Hydraulic Load Frame.....	30
Figure 12. Location of Tissue Dye Marks.....	31
Figure 13. Impaction Apparatus.....	31
Figure 14. Patella in Impaction Apparatus.....	32
Figure 15. Patella Incubation.....	33
Figure 16. Tissue Preparation and Freezing.....	35
Figure 17. Impact Geometry.....	37
Figure 18. A Collective Montage (MTT stained).....	38
Figure 19. Tissue Column (10 regions).....	39
Figure 20. A Collective Montage (Safranin-O stained).....	40
Figure 21. Mean Percentage of Dead Cells.....	43

Figure 22. Percentage of Dead Cells by Tissue Depth.....	45
Figure 23. Percentage of Dead Cells by Radial Position.....	46
Figure 24. Mean Normalized Intensity by Tissue Depth.....	48
Figure 25. Normalized Intensity by Tissue Depth.....	50
Figure 26. Normalized Intensity by Radial Position.....	51
Figure 27. Live and Dead Chondrocytes.....	56
Figure 28. Cell Clusters.....	57

## 1 Introduction

The overall goal of this research was to examine the response of articular cartilage following a mechanical impact injury, as a model for the development of osteoarthritis. An *in-vitro* model of cartilage degeneration was developed to examine the timing of early degenerative changes; and to correlate applied mechanical stress with the biochemical pathways that lead to matrix degradation. The focus of this part of the study was to determine the timing of chondrocyte death and proteoglycan loss over the first two weeks following an impact injury.

Osteoarthritis is a severely debilitating disease that affects the cartilage layer and bone of joints, causing them to degrade over time. It is a slowly progressing and chronic disease whose exact process is unknown. During normal everyday activities, mechanical loads are transmitted between articular cartilage surfaces, such as the patella-femoral joint. However excessive mechanical loading of diarthrodial joints, as occurs with injury or trauma, may often be an initiating factor for cartilage degeneration and can lead to severe conditions such as osteoarthritis.<sup>14,17,18,31,44,56,59</sup> Although it is thought that age, sex, racial characteristics and genetics establish the foundation for cartilage properties, many other biomechanical factors can influence the degradation of articular cartilage. These biomechanical factors include occupation, obesity, overuse, degree of joint loading and injury.<sup>4</sup>

While the final stages of osteoarthritis are quite well documented, the early tissue changes that start the tissue down the degenerative pathway are yet to be understood. In order to gain a better understanding of how cellular and matrix changes influence the progression of degenerative diseases, it is necessary to observe their time-dependent behavior

in response to a stimulus known to be a predisposing factor for such diseases, traumatic injury.

## 2 Cartilage

There are three types of cartilage: fibrocartilage, which is the transitional cartilage found at margins of some joint cavities and insertions of ligaments and tendons to bone (i.e. menisci and annulus fibrosis), elastic cartilage (found in the external ear, epiglottis and larynx) and articular cartilage.<sup>40</sup> Articular cartilage (Figure 1) is the type of cartilage found in joints that lines the ends of bones and completes the rib cage.<sup>7</sup>

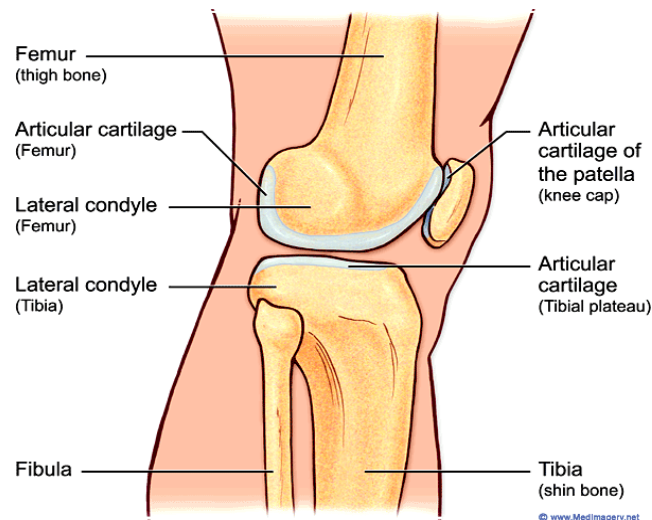


Figure 1. The Knee Joint (and associated articular cartilage).<sup>38</sup>

## 3 Articular Cartilage

Articular cartilage is a highly specialized biomaterial that has two primary functions: to distribute joint loads over a wide area in order to decrease stresses experienced by the contacting joint surfaces, and to allow relative movement of opposing joint surfaces with minimal friction and wear, providing a smooth, low friction surface for joint articulation. As

shown in Figure 2, articular cartilage in its young, normal and healthy state it appears glassy, smooth, glistening and bluish white to the naked eye.<sup>40,46</sup>

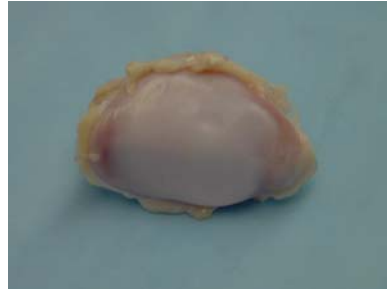


Figure 2. A Porcine Patella (showing a healthy articular cartilage surface).

Unlike bone, cartilage has very little capacity for regeneration in adults. Adult human articular cartilage is avascular, therefore there is no external cell supply to compensate for cell loss caused by apoptosis, necrosis or other cellular mechanisms.<sup>1</sup> The little healing that does take place is due to the ability of the surviving chondrocytes to secrete more extracellular matrix.<sup>7</sup>

### 3.1 Joint Tissue Structure and Composition

Articular cartilage is divided into 3 major zones: the superficial/tangential zone is comprised of the top 10%-20% of the cartilage layer, followed by the middle/transitional zone (40%-60%) and deep/radial zone (30%-40%).<sup>46</sup> A microscopically distinct line called the tidemark, separates the deep zone from the underlying calcified cartilage; deep to the calcified region lies the subchondral plate of bone (Figure 3).<sup>19,53</sup> This layer of underlying bone is known to constrain the cartilage and has been suggested to have a protective effect on the cartilage matrix during loading. Thus the removal of the cartilage from the bone would likely alter the state of stress in the cartilage.<sup>18,25</sup>

Each zone in the cartilage is distinguished by the shape of the chondrocytes, the content of proteoglycans and the arrangement of the type II collagen fibers (Figure 3), which will be covered in the subsequent sections.

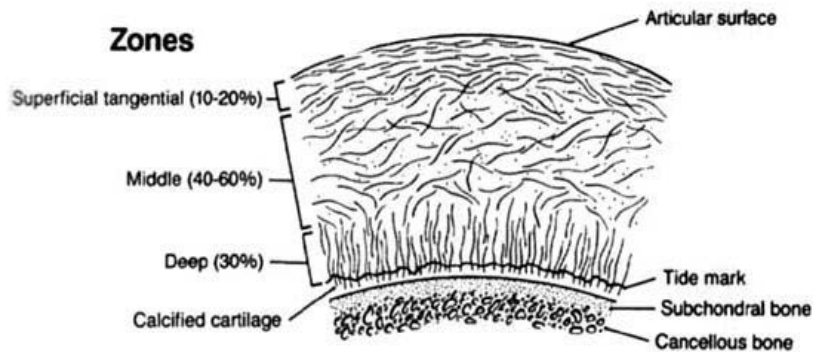


Figure 3. The Zones of Articular Cartilage (and the distribution of type II collagen fibers).<sup>40</sup>

The shape and composition of these cartilage components depend on the type of load that the tissue experiences. The intrinsic mechanical properties of articular cartilage vary with depth. For example, the superficial zone of articular cartilage is softer and less permeable than the regions below,<sup>52</sup> in adaptation to the shear stress from motion.

### 3.2 Matrix Components

To support body weight at rest and during activity, articular cartilage must be able to withstand the compressive forces that the joints experience. Two major matrix macromolecules help to provide this function: proteoglycan (PG) and collagen.<sup>42</sup> These components, along with water, combine to impart to cartilage its macroscopic material properties. Articular cartilage is regarded as a biphasic material, with two major phases: a fluid phase composed of water and electrolytes, and a solid phase composed of collagen, proteoglycans and other proteins, glycoproteins and cartilage cells (or chondrocytes).<sup>46</sup> Type

II collagen accounts for approximately 75% dry tissue weight and proteoglycans are approximately 20%-25% of the dry tissue weight.<sup>32</sup> Both proteoglycan and collagen together make up about 25% of the wet weight of cartilage, with water accounting for the remainder.<sup>48</sup> In general the interaction of water, proteoglycans, collagen and chondrocytes within the matrix depend on the type of cartilage (i.e. articular or fibrous) and the loads and deformations that the tissue experiences.<sup>46</sup>

### **3.3 Proteoglycans**

Cartilage PG's are inhomogeneously distributed throughout the matrix, with their concentration generally being lowest in the superficial and deep zones and highest in the middle zone.<sup>40</sup> The distribution of this macromolecule reflects the ability of articular cartilage to resist compression.

The basic structural unit of the proteoglycan macromolecule is aggrecan. In the matrix the predominant monomer, aggrecan, noncovalently binds to hyaluronan and a link protein stabilizes this interaction between the binding region to form the PG macromolecule (Figure 4).<sup>40</sup> Aggrecan consists of a central protein core with many covalently attached, negatively charged glycosaminoglycans (GAGS), for example,  $\text{SO}_3^-$  and  $\text{COO}^-$ . GAGS are chains of repeating disaccharide units that attract water molecules. GAGS in cartilage include chondroitin sulphate and keratin sulphate (Figure 4).<sup>27,39,40</sup>

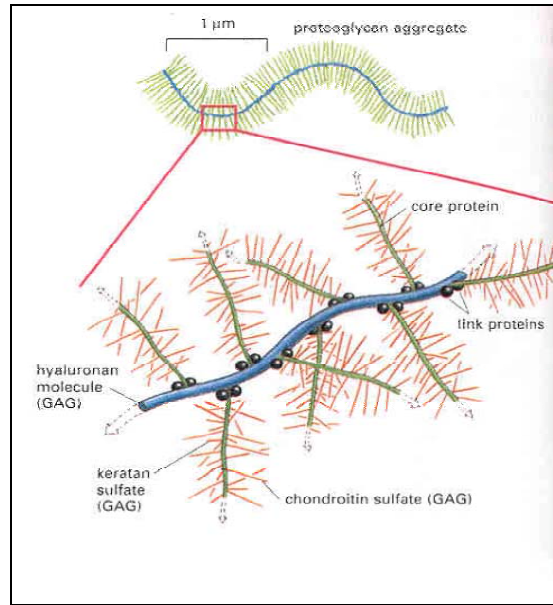


Figure 4. A Proteoglycan Molecule<sup>10</sup>

The negative electrical charges of chondroitin and keratin sulphates cause them to repel each other. The highly sulphated GAG content of proteoglycan attracts water molecules and hence allows the tissue to swell and resist compressive forces. This is known as the Donnan osmotic swelling pressure.<sup>40</sup>

The interaction between collagen, PG and water is believed to have an important function in regulating the structural organization of the extracellular matrix. Cartilage absorbs water when there is no pressure exerted upon the joint and squeezing out water when pressure is applied on the joint. That is, when loaded by a compressive force, the internal pressure in the matrix exceeds the osmotic swelling pressure, causing fluid to flow out of and through the tissue. As the fluid flows out, the PG concentration increases. Intermolecular charge-charge repulsive forces develop that tend to extend and stiffen the PG macromolecules, enabling cartilage to resist compression.<sup>40</sup> If loading continues, water flow through the porous matrix takes place causing extra strain or stress relaxation. This process



depends on the cartilage permeability, which is primarily influenced by the PGs.<sup>4</sup> However if loads are applied so quickly that there is insufficient opportunity for fluid redistribution to the compressed region, the high stresses produced in the collagen-PG matrix may induce damage.<sup>40</sup> An example of this is an injury that occurs due to an impact load.

### **3.4 Type II Collagen**

A variety of different collagen (types V, VI, IX, XI) can be found in quantitatively small amounts in articular cartilage, however type II collagen is the most abundant.<sup>40</sup> The collagen are tough fibers which are laid down in a crisscross pattern to create a framework that contains the proteoglycans. In the superficial tangential zone, the collagen fibers are oriented parallel to the articular surface. For example, if the surface of articular cartilage is pierced by a pin, and then withdrawn, a longitudinal “split line” appears. The pattern of split-lines shows the predominant direction of the collagen fibers in the cartilage.<sup>20</sup> Collagen fibers in the middle zone are less densely packed and more randomly oriented (as opposed to the same direction). In the deep zone, the fibers are perpendicular to the articular surface, crossing the tidemark (or boundary between the calcified and noncalcified tissue) and anchoring the tissue to the bone (Figure 3).<sup>46</sup>

The basic unit of a collagen fiber is tropocollagen, a structure composed of three procollagen polypeptide chains (alpha chains) coiled into left-handed helices that are further coiled about each other to form a right-handed helix.<sup>46</sup> Specifically, the three procollagen molecules synthesize to form the tropocollagen triple helix (Figure 5). These tropocollagen chains then assemble and cross-link to form a collagen fibril. The fibrils then group to form a collagen fiber. The proteoglycans are anchored in spaces in the collagen fiber network that constrains the expansion of the PG molecules.<sup>48</sup>

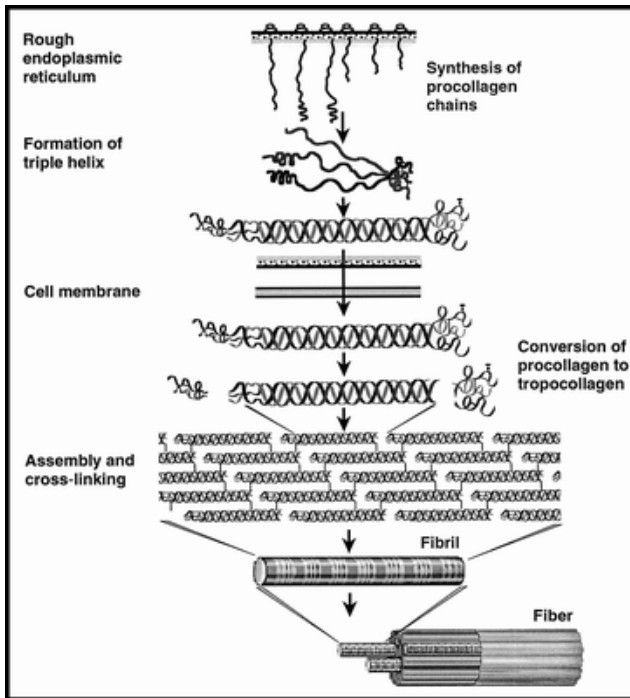


Figure 5. Synthesis, Secretion and Assembly of a Collagen Fiber<sup>49</sup>

The most important mechanical properties of collagen fibers are providing tensile and shear strength to the cartilage.<sup>4,40</sup> Collagen offers little resistance to compression. Because of their large ratio of length to thickness, collagen fibers can easily buckle under compressive loads.<sup>40</sup> Since articular cartilage is anisotropic, meaning that its material properties differ with the direction of load, it is thought that the variations in collagen-proteoglycan interactions help create the cartilage tensile anisotropy.<sup>40</sup> For example, osmotic pressure exerted by  $\text{SO}_3^-$  and  $\text{COO}^-$  charge groups along the GAGs permits the PG in the collagen network to swell and resist compression, therefore helping maintain the ECM organization. This swelling behavior is constrained by the collagen network thus placing it under tension. This also provides shear stiffness to the ECM.<sup>46</sup>

### **3.5 Chondrocytes**

The articular cartilage extracellular matrix is synthesized by the resident cells, the chondrocytes. These cells are responsible for synthesizing and maintaining the proteoglycan and collagen of the solid matrix.<sup>26</sup> They can also produce several mediators that have the potential to induce chondrocyte death through apoptotic or necrotic pathways. Among these mediators are cytokines (e.g. IL-1), tumor necrosis factor (TNF), oxygen radicals, enzymes and nitric oxide.<sup>23,24</sup> Although the important roles of a chondrocyte include the synthesis and maintenance of the matrix, the turnover rate is very slow.

In normal cartilage, chondrocytes are sparsely distributed throughout the extracellular matrix.<sup>53</sup> In the superficial tangential zone, chondrocytes are oblong in shape with their long axes parallel to the articular surface. In the middle zone they are round in shape and randomly distributed and in the deep zone, they are arranged in a vertical columnar fashion.<sup>40</sup>

Chondrocytes are surrounded by a tissue region which investigators have called the 'pericellular' matrix, which contains large amounts of type VI collagen and a high concentration of proteoglycan. The chondrocyte together with the pericellular matrix is called the 'chondron' (Figure 6).

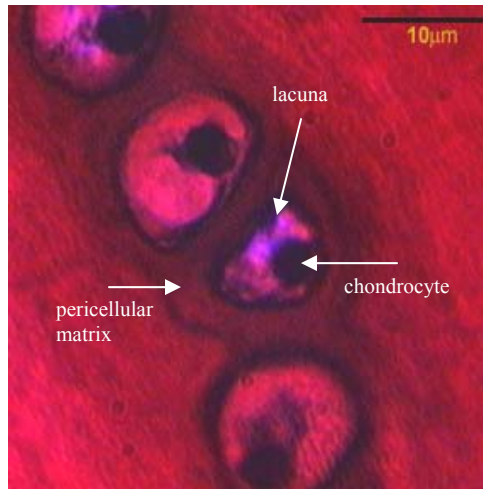


Figure 6. An Articular Cartilage Chondron

Little is known about the exact functional significance of the chondron. However, since the pericellular matrix completely surrounds the chondrocyte, it is possible that biochemical or biophysical signals that the chondrocyte receives are influenced by this region. One approach in determining the role of these signals is to assess the mechanical environment of the chondrocyte under physiological loading.<sup>21</sup> For example, a study by Clark *et al.*, using feline cartilage attached to its subchondral bone, applied a uniform static loads of 9 and 15 MPa (corresponding to a peak patellofemoral contact force of 170 N which occurs during normal gait).<sup>11</sup> They discovered significant changes to chondrocyte shape and volume. Other studies have observed reductions in nucleus volume and height, a reduction in aggrecan synthesis and an enlarged chondron area in osteoarthritic cartilage, thus demonstrating that chondrocytes respond to changes in their physical environment within the ECM as injury progresses. This is an important factor in the survival and function of the cells and ultimately their associated cartilage and joint.<sup>11,21</sup>

#### 4 Osteoarthritis

Osteoarthritis (OA), a degenerative joint disease, occurs when there is disruption of normal cartilage structure and homeostasis (Figure 7). It is the leading cause of arthritis in the United States and affects an estimated 21 million Americans.<sup>3</sup> Unlike rheumatoid arthritis, which usually affects the respective joint symmetrically (i.e. both knees, both hands etc.), OA often occurs in one joint with different pathology in its symmetrical equivalent. It is characterized by the degradation of cartilage protecting the ends of articulating bone joints, erosive cartilage lesions and subchondral bone sclerosis and cysts.<sup>12,26,46</sup>

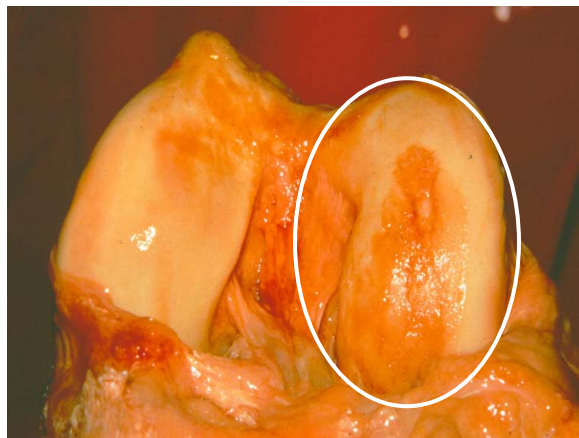


Figure 7. Osteoarthritic Cartilage (at the distal end of the femur), indicated by the circle.

OA falls into two categories: Primary (or idiopathic) OA occurs in middle-aged to elderly patients where the progression of the disease is often presumed to be a consequence of joint ‘wear and tear’. In primary OA, degeneration is first observed at the articular surface in the form of fibrillation where the disease process may take as long as 15-20 years. Secondary OA can occur at any age as a result of trauma or disease.<sup>48</sup> In

secondary or post-traumatic OA, degenerative changes may involve the entire articular cartilage. Matrix changes are detectable within days or weeks following joint injury such as damage to the meniscus or surrounding ligaments.<sup>43</sup> In both cases, the central feature is loss of articular cartilage, a reduced capacity for repair, joint dysfunction,<sup>23,48</sup> and damage to the surrounding bone tissue.<sup>43</sup> Changes associated with OA ultimately have an impact on the patient through a decreased ability to use the joint and/or the production of pain due to increased articular surface friction during motion, causing increase heat production and tissue inflammation.<sup>26</sup>

#### **4.1 Proteoglycan Content and Osteoarthritis**

Decreases in PG concentration, collagen network disorganization, and softening of the tissue are the early signs of cartilage injury and OA. Proteoglycan depletion is probably not sufficient to initiate cartilage destruction, thus injury of the collagen network in the cartilage surface is necessary.<sup>4</sup> Prior studies have noted that injury and excessive impact loading can produce structural damage and osteoarthritic-like changes including tissue swelling, increased collagen denaturation and reduced proteoglycan synthesis in cartilage explants.<sup>9,29</sup> Since swelling is a result of electrostatic repulsion of charged proteoglycans, and opposed by the collagen network, swelling of the tissue after injury is thought to indicate damage to the collagen network.<sup>29</sup> Therefore proteoglycan loss and perturbation of the collagen network provide an ideal environment for the disturbance of chondrocyte anchorage to the extracellular matrix, interfering with proper cellular growth, function and survival.<sup>1</sup>

#### **4.2 Chondrocyte Death and Osteoarthritis**

Chondrocyte death is a major factor contributing to the degeneration of articular cartilage.<sup>1,2,14,18,23,24,34,36,47,48,50,54,</sup> In osteoarthritis, cartilage degeneration is largely a

process of destruction and failure of the extracellular matrix which serves as the functional component of connective tissues. Since chondrocytes are the only source of matrix component (i.e. collagen and proteoglycans) synthesis, it has been suggested that the failure of the cartilage matrix can implicate a failure of the involved cells.<sup>1,14</sup> On the other hand, studies have also found that disturbance of the cartilage matrix may expose the chondrocytes to mechanical stress, leading eventually to cell death.<sup>34</sup>

In tissues other than cartilage, mononuclear phagocytes are responsible for ingesting and disposing of dead cells. However, the absence of these phagocytes in cartilage implies that the remnants of dead cells remain in the matrix and potentially affect matrix structure and the function of viable chondrocytes.<sup>35</sup> Furthermore, since chondrocytes are anchored in the extracellular matrix and are surrounded by a pericellular matrix, there is no apparent mechanism for the clearance of damaged or dead cells.<sup>23,24</sup> Many studies have shown that there is a very low proliferative activity (also known as cell cloning) in OA chondrocytes resulting in cell clusters typical of OA cartilage.<sup>2,54</sup> However it is doubtful that this is a mode of tissue repair since they do not appear to add to matrix anabolism.<sup>1</sup>

### **4.3 Apoptosis and Necrosis**

Studies have shown a decrease in (viable) chondrocyte numbers in osteoarthritic cartilage, which may be a result of apoptosis or other forms of cell death like those induced by injury, such as necrosis (Figure 8).<sup>9,23,54</sup> Apoptosis is a programmed cell death, where an internal death program is activated in the cell that leads to a chain of events, which includes condensation of the cytoplasm and nucleus by internucleosomal cleavage of DNA.<sup>1,9,37</sup> Studies have reported apoptotic cells to be shrunken in appearance, with blebbing of the

cytoplasmic membrane and absence of the pericellular matrix (i.e. retracting from the surrounding matrix).<sup>23,24,41</sup> Necrosis encompasses all forms of programmed and non-programmed cell death, however the term is commonly used for non-programmed or pathological cell death. Necrosis usually occurs in a localized area and typically results from exposure to cytotoxic chemicals or cell trauma, as occurs in an impact injury. It is characterized by a leaky or ruptured cell membrane (with a general lack of membrane integrity) and amorphous granular debris throughout the lacunae and matrix border.<sup>1,9,37,41</sup>

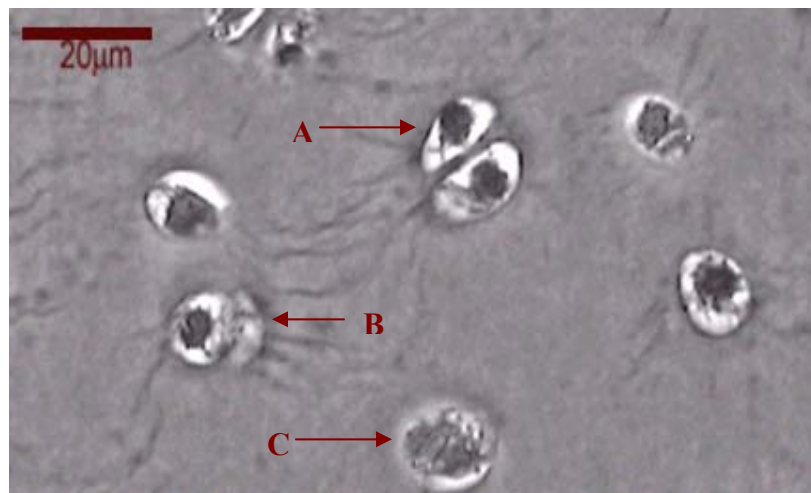


Figure 8. Articular Cartilage Chondrocytes. A. a viable cell B. a cell with characteristics of necrosis, and C. a cell with characteristics of apoptosis.

Excessive mechanical loading has been identified as an important factor responsible for the reduced chondrocyte viability.<sup>9,25,34,36,50</sup> After performing cyclic indentation impacts on articular cartilage, Chen *et al.*<sup>9</sup>, found that in cartilage that had been loaded for 2 hours, 32% of the chondrocytes demonstrated the leaky cell membranes (characteristic of necrosis) in the middle to superficial zones. After 4 hours, less than 1% the cells were positive for apoptosis. The apoptotic cells increased to 73% after 2 days in culture. It was concluded that the first mode of cell death in the cartilage after repeated impacts was most likely



necrosis (even though some evidence apoptosis occurred).<sup>9</sup> However the mode of cell death in injured and diseased cartilage may be a mixture of necrosis and apoptosis.

A study conducted by S.Hashimoto *et al.*<sup>23</sup>, examined the occurrence of apoptosis in human OA cartilage to determine its relationship to cartilage degradation. After examining normal and OA human cartilage, they found that apoptotic cells were surrounded by a matrix that showed proteoglycan depletion. In contrast, areas that had no apoptotic cells showed normal proteoglycan content.<sup>23</sup> Another study by Quinn *et al.*<sup>45</sup>, observed general cell death and decreased matrix proteoglycan deposition near the articular surface for both low and high strain rates of loading.

## **5 Models of Cartilage Degeneration**

Injury or mechanical loading of articular cartilage has been shown to be a major predecessor to degenerative changes associated with osteoarthritis.<sup>4,8,9,14,18,22,23,24,29,34,42,50,58</sup> Although loads and forces applied to joints during daily activity have important influence on cartilage metabolism and structure, the stresses due to trauma, joint overuse and obesity may lead to cartilage degeneration.<sup>4,44</sup> Many studies have attempted to simulate such loads in order to understand the pathways leading from joint injury to OA. However the progression to the disease is still not well understood.

### **5.1 Techniques for Experimental Loading of Cartilage**

Several investigators have studied the outcome of damaged cartilage using either *in vivo* animal models of joint trauma,<sup>15,56,58</sup> or by monitoring the changes after *in vitro* mechanically induced tissue trauma.<sup>6,31,25,28,42,59</sup> Although *in vivo* models provide a more realistic environment to follow subsequent tissue and cellular changes, they tend to be problematic due to difficulties in repeatability and accurate correlation of damage to loading. *In vitro*

models provide better control over the loading, are simpler and allow for a greater number of samples to be run. A disadvantage to this technique is the risk of additional damage to the explant as it is removed from the joint. In addition, the removal of the cartilage tissue from the bone has been shown to significantly affect the mechanical behavior of the tissue.<sup>25</sup>

Techniques for *in vitro* mechanically induced cartilage degeneration have included cyclic, compressive and impact loading.<sup>6,44</sup> Cyclic or repetitive loading may simulate abnormal loads applied during locomotion. Compressive or sub-impact loading imitates weight-bearing in misaligned joints as in obesity or some sports activities. Single impact loads may simulate acute joint trauma that occurs in automobile accidents or sport injuries. These blunt impact injuries occur at a much more rapid rate than that of compressive loads (which evolve over seconds or more).<sup>44</sup> Although *in vitro* model systems of mechanical loading do not accurately reflect what happens in human articular cartilage in everyday life, they provide an excellent means for explanation for the increased risk of OA posed by joint overloading.<sup>1</sup>

## **5.2 *In vitro* Impact Models of Articular Cartilage: Literature Review**

The mechanical impaction protocols of *in vitro* models of articular cartilage injury vary between studies. Most studies utilize either a chondral explant (with the cartilage tissue removed from the bone) or an osteochondral explant (with the cartilage attached to the bone), and expose the specimen to impact loads in unconfined compression. A study conducted by Jeffrey *et al.*,<sup>25</sup> impacted both bovine chondral and subchondral biopsies to masses of 100 g and 1 kg from a drop tower device at heights of 5, 10, 20 and 50 cm. A 500 g mass was also dropped from heights of 5, 10, 20 and 50 cm. It was found that the mass of the explants reduced to 60% and chondrocyte viability fell to 40% of their preimpacted value for samples

loaded with the 500 g mass from 20cm. Cell viability was unaffected by moderate impacts but decreased linearly with increasing impact energy for all samples. The extent of damage through the depth of the tissue was much more severe for chondral samples than for samples left attached to the underlying bone during impact. The findings suggest that cartilage is very resistant to impact loads provided the bone-cartilage interface is intact, showing the underlying bone to have a strong protective effect.

A similar protocol was used in a study conducted by Krueger *et al.*,<sup>28</sup> that subjected both chondral and osteochondral explants to a 30 MPa load at either a high rate of loading (600 MPa/s) or a low rate of loading (30 MPa/s), with the intent of determining whether the presence of underlying bone affects the degree of dead cell distribution. After 24 hours in culture, the results revealed that more matrix damage and a higher amount of cell death in all zones was seen in chondral explants than osteochondral explants at the low loading rate. At the high rate of loading, the percentage of cell death was lower in the intermediate and deep zones of the osteochondral explant. Therefore the presence of underlying bone had an affect on the cell death distribution and limited the degree of cell death and matrix damage through the thickness of the explant.

Studies using osteochondral explants at high rates of loading have documented cell death adjacent to surface lesions. In contrast, studies involving explants removed from the bone at low rates of loading suggest no clear spatial association between cell death and matrix damage.<sup>18</sup> These two types of studies exhibit inconsistent results with respect to cell death and matrix damage. Therefore the loading rate and magnitude of the load are important factors to consider when investigating damage in mechanically impacted cartilage. In Ewers *et al.*'s study,<sup>18</sup> bovine cartilage explants were subjected to unconfined compression

at either a high rate (~900 MPa/s) or a low rate (40 MPa/s) of loading to a peak load of 1247N (40 MPa) and cultured for 4 days post-loading. Gross observations indicated surface fissures only in the top surface for all loaded explants with cell death appearing to be adjacent to fissures for specimens subjected to the high load rate. Results revealed that the number of dead cells and percentage of dead versus live cells were significantly higher and distributed more diffusely in explants subjected to the low rate of loading. After two days, the amount of GAG released to the media from explants subjected to the high rate of loading was significantly greater than that released from specimens exposed to the low rate of loading, indicating a possible increase in matrix damage. These results imply that the higher cell death in the low loading rate group may have caused a cell-mediated degradation of proteoglycans, however it was unclear if the GAG loss represented cell-mediated degradation or a direct loss due to matrix damage. There were no significant differences after three days post-culture. The study concluded that in unconfined compression experiments on cartilage explants, the rate of loading can significantly affect the degree of matrix damage, the distribution of dead cells and the amount of cell death.

Another study, which was also performed by Ewers *et al.*,<sup>17</sup> examined affects of the rate of blunt impact loading on retropatellar cartilage and underlying bone in rabbit patella. The protocol involved a flat impactor dropping a 1.33 kg mass from 0.46 meters to create a blunt impact to the patellofemoral joint with a high rate of loading (~ 5ms to peak) versus a low rate of loading (~ 50ms to peak). Animals were sacrificed 12 months post-impact and patellae were excised for mechanical indentation tests using a non-porous probe. Results showed that the low rate experiments resulted in a 24% increase in subchondral bone thickness at the central site compared to control patellae. The high rate impacts resulted in

an increase in surface fissures and a 29%, 60% and 44% increase in thickness under the lateral, central and medial sites respectively, compared to the low rate of loading. This experiment concluded that the rate of impact loading may be a highly important factor in determining the mechanisms of chronic retropatellar cartilage injury.

A flat impactor was also used in a study by Lewis *et al.*,<sup>31</sup> to examine cell death after impact, as a function of spatial location and time. The articular surface of whole, intact, mature bovine patellae, were impacted at 6000 N/s to a target peak load of 1500 N (53 MPa in 250 ms). Cartilage sections were removed from the bone and placed in culture groups of 18 hours and 5 days post-impact and the cartilage was divided into four zones of equal depth through the cartilage layer. The greatest loss of cell viability was in the surface zone, but the statistically significant difference was found in zones 1 and 2 and there was no statistical difference between the 18 hour and 5 day values in any zone due to impact. At 5 days, cell death increased in the surface layer in both the control and impacted tissue. There was no difference in cell viability in impacted regions away from visible cracks compared to non-impacted controls. A decrease in viable cell density was seen to be localized only in specimens with macroscopic matrix cracks. Therefore cell death after impaction of cartilage on intact patellae occurred around impact induced cracks and not in impacted areas without cracks.

Unlike the previously described study, many investigators prefer to use curved or contoured impactors to perform direct impacts to the articular cartilage surface. An experiment was performed by Zhang *et al.*,<sup>59</sup> to evaluate the extent of gross and histological damage to femoral articular cartilage and subchondral bone caused by different impactor types, magnitudes of impact force and impact stress. Twelve rabbit knees were divided into

three groups and exposed to *in vitro* impacts of uniform stresses from a drop tower height of 40 cm: four knees had a 350 g mass dropped onto a contoured impactor, four knees had a 1050 g mass dropped onto a contoured impactor and four knees had a 1050 g mass dropped onto a flat impactor. Gross examination indicated that contoured impactors produced superficial fibrillation (and progressed deeper as impact stress increased) while flat impactors produced deep cracks in the tissue. Histologically, the severity of damage correlated with the magnitude of the impact force, where impact forces above 500 N created more damage than impact forces below 500 N. None of the specimens showed any injury or damage to the subchondral bone. It was concluded that flat impactors are best used to study localized impact damage while contoured impactors are ideal if the goal is to study diffuse cartilage damage or stress effects.

In a study conducted by Quinn, *et al.*,<sup>45</sup> sub-impact loads were applied to bovine osteochondral explants with an impermeable loading post (10 mm in diameter) at a constant strain rate between  $3 \times 10^{-5}$  and  $0.7 \text{ s}^{-1}$  to a peak stress between 3.5 and 14 MPa and maintained in culture for four days. For low strain rate, results indicated a large region of deactivated (dead) cells observed near the central region of explants for all depths from articular surface at 7 MPa peak stress. Extensive to total cell death was observed for all depths in 14 MPa peak stress. Cell death at higher strain rates were most severe near the superficial zone and were associated with increased proteoglycan release. Loading conditions lower than 14 MPa or lower than  $0.5 \text{ s}^{-1}$  strain rate showed no significant proteoglycan release compared to controls. The findings for the low strain rate are similar to values obtained in studies involving static compression and results from the high strain rate are similar to that which occurs in impaction studies. Therefore it is not likely that the nature

of injury (i.e. impact versus sub-impact) will be evident among non-physiological joint loading histories.

Similarly, other studies have also observed cell death and proteoglycan depletion mainly in the superficial zone of cartilage. A study using both osteoarthritic and healthy human articular cartilage was conducted by Hashimoto *et al.*<sup>23</sup> Immediately after removing cartilage samples from the femoral condyles, the number of apoptotic chondrocytes was analyzed using flow cytometry. It was found that the high frequency of apoptotic cells in the superficial layer correlated with the most severe loss of proteoglycan in this area. Similarly, Lafeber *et al.*,<sup>30</sup> also compared osteoarthritic and healthy human knee cartilage. After 4 days in culture, a lower rate of proteoglycan synthesis was seen in OA cartilage compared to normal cartilage in the superficial cartilage layer. Also, chondrocytes in the superficial zone of osteoarthritic cartilage (compared to normal cartilage) were mainly joined in cell clusters and proliferating. It was suggested that the proliferative activity may have caused the inability of the chondrocytes to contribute to proteoglycan synthesis.

In Triantafillopoulos *et al.*'s experiment,<sup>56</sup> traumatic injury was experimentally induced *in vivo* on patella of 45 New Zealand rabbits by dropping a falling weight (approximately 750g or 6 J) through a cylindrical pipe from a height of 1m onto the contoured impactor that rested on top of the patella. After 1 to 15 days and at 1-3 months after injury, animals were sacrificed and articular cartilage of patella was observed. By day 4 after injury, light microscopy findings showed cell death progression from superficial to the deep layer. At 8 days, proliferation of chondrocytes was observed in all cartilage layers, especially in the middle layer. Chondrocyte proliferation decreased gradually at 30, 60 and 90 days. Characteristic osteoarthritic changes like decreased cellular density, empty lacunae

and cell cluster formations were observed. Control patellar specimens were free from histopathological changes. Similar results were seen in Tew et al's study,<sup>54</sup> where initial cell death was seen at the lesion edge of a cartilage wound created by a trephine. By day 5 post-injury, a proliferative cell response was seen subsequent to the cell death. These findings suggest that the impaction of articular cartilage was the initiating factor for progressive osteoarthritic-like changes, but the damage progression or repair mechanisms require further investigation.

## **6 Purpose of Study**

The prevailing view is that osteoarthritis starts from the cartilage surface through PG depletion and fibrillation of the superficial collagen network. It has also been suggested that the initial structural changes take place in the subchondral bone, especially when the joint is subjected to an impact type of loading.<sup>4</sup> Several studies on the correlation between mechanical injury and cartilage viability have demonstrated that blunt impact trauma can lead to morphological and cellular damage to cartilage,<sup>14</sup> similar to that seen in degenerative joint diseases such as osteoarthritis. There are contrasting outcomes with respect to matrix changes and cell viability, depending on the size and shape of the impactor, the type of explant (chondral versus osteochondral), the time in culture, the nature of the injury model and the method of tissue analysis. Few studies have examined the time-related changes in chondrocyte viability and proteoglycan content, using an intact patella, with respect to tissue depth and radial position from the impactor. It is still unclear how the interaction of these components can contribute to early cartilage degeneration. In addition most studies have not cultured specimens for more than 7 days and many studies have only assessed tissue changes in advanced osteoarthritis. Temporal and spatial investigations of the early matrix and



cellular changes that herald the beginning of osteoarthritis and how these critical changes may lead to articular cartilage degradation and advanced osteoarthritis are yet to be conducted. The goal of this research is to study the changes in chondrocyte viability and proteoglycan concentration relative to the magnitude of an impact injury, time following the injury, and relative location within the cartilage layer. If the occurrence of these degenerative events can be identified temporally, it may represent a window of opportunity for intervention. Therefore such studies will not only contribute to existing knowledge but will also help create new and improved treatments and intervention therapies for conditions such as osteoarthritis.

### **6.1 Hypotheses**

Subjecting articular cartilage to injurious mechanical loads (similar to an injury) will result in chondrocyte death and proteoglycan depletion. The cellular matrix changes will be dependent on the magnitude of load, days in culture and the position in the tissue related to the center of impaction.

Mechanical injury of normal porcine articular cartilage will result in a higher incidence of cell death compared to non-impacted controls. Cell death will occur initially at the superficial zone for medium loaded cartilage, and at both superficial and deep zones for high loads. Cell death will occur initially in the center of impaction and will continue outward toward the adjacent radial positions over time.

Injury will result in more proteoglycan depletion at high load levels because impact loads will squeeze out water so quickly that there is would be insufficient opportunity for fluid redistribution to the compressed region,<sup>40</sup> making the proteoglycans and other matrix components vulnerable to damage.

## **7 Methods**

In this study, paired porcine knee joints from adult pigs were obtained fresh from a local slaughterhouse. The cartilage of the patellae were injured with a single impaction of high load (2000 Newtons) or medium (1000 Newtons) load level to the articular surface. Degenerative changes were followed after entire patellae were placed, intact, into culture for a time period of 0, 3, 7, or 14 days. Two different analyses using light microscopy were performed through the depth of the articular cartilage tissue on the impacted sites for: (1) measurement chondrocyte death, and (2) measurement proteoglycan distribution.

### **7.1 Randomization of Specimens**

Patellae were randomly assigned a culture time and impaction load level using a balanced incomplete block design with Excel software (Table 1). For each loading condition (control = no load, medium = 1000 N, and high = 2000 N), each culture time (0, 3, 7 and 14 days) was paired with the other three using paired left and right patellae.

Table 1. Randomization of Specimens

<b>Right Leg</b>	<b>Left Leg</b>	<b>Randomization</b>
M3	M14	0.012737
H0	H3	0.06598
C7	C14	0.075959
H0	H14	0.196122
M0	M3	0.205526
C0	C7	0.213661
C3	C7	0.254995
M7	M14	0.298631
H7	H0	0.326353
H3	H7	0.328928
C3	C14	0.521827
C14	C0	0.572349
H3	H14	0.612532
C0	C3	0.622903
M0	M7	0.681366
M3	M7	0.855188
H7	H14	0.885797
M14	M0	0.906083

Table 2. Impaction Groupings – paired left and right patella from the same animal.

No Load		Medium Load		High Load	
Right	Left	Right	Left	Right	Left
0	3	0	3	0	3
0	7	0	7	0	7
0	14	0	14	0	14
3	7	3	7	3	7
3	14	3	14	3	14
7	14	7	14	7	14

This created a block of 9 patellae at each load level and 3 at each culture time, resulting in a total of 36 patellae (Table 2). Force levels necessary to obtain damage levels were determined before testing started. Patellae were removed from the knee joint and impacted in order from right to left. Specimens were assigned names that specified the impact level

(C, M or H), time in culture (0, 3, 7, or 14), knee (R or L), facet (M or L) and type of load (i.e. axial) (Table 3).

Table 3. Schedule of Experiment Dates and Associated Specimens

TEST DATE	ORDER	LOAD	CULTURE TIME	LEG	SPECIMEN NAME
06/13/03	1	Medium	7	Right	M7RMax
	2	Medium	14	Left	M14LMax
	3	High	7	Right	H7RMax
	4	High	0	Left	H0LMax
07/01/03	5	High	3	Right	H3RMax(a)
	6	High	7	Left	H7LMax
	7	Control	3	Right	C3RMax
	8	Control	14	Left	C14LMax
	9	Control	14	Right	C14RMax
	10	Control	0	Left	C0LMax
	11	High	3	Right	H3RMax(b)
	12	High	14	Left	H14LMax
07/29/03	13	Control	0	Right	C0RMax
	14	Control	3	Left	C3LMax
	15	Medium	0	Right	M0RMax
	16	Medium	7	Left	M7LMax
	17	Medium	3	Right	M3RMax
	18	Medium	7	Left	M7LMax
08/12/03	19	High	7	Right	H7RMax
	20	High	14	Left	H14LMax
	21	Medium	14	Right	M14RMax
	22	Medium	0	Left	M0LMax
09/12/03	23	Medium	3	Right	M3RMax
	24	Medium	14	Left	M14LMax
	25	High	0	Right	H0RMax
	26	High	3	Left	H3LMax
10/03/03	27	Control	7	Right	C7RMax
	28	Control	14	Left	C14LMax
	29	High	0	Right	H0RMax
	30	High	14	Left	H14LMax
	31	Medium	0	Right	M0RMax
	32	Medium	3	Left	M3LMax
10/10/03	33	Control	0	Right	C0RMax
	34	Control	7	Left	C7LMax(a)
	35	Control	3	Right	C3RMax
	36	Control	7	Left	C7LMax(b)

## 7.2 Porcine Patella Removal

Prior to extracting the patellae from the knee joints, all utensils and objects coming in contact with the specimens were steam sterilized in an autoclave at 121°C for 55min gravity cycle and 60min dry time. Sterile sheets were placed on countertops cleaned with 70% Ethyl Alcohol. Starting with a right knee, each knee was sprayed with betadine and wiped with a

sterile cotton pad, followed by spraying with 70% EtOH. The knee was then transferred onto a fresh sterile sheet. Sterile gloves and surgical gowns, along with protective eyewear and facemasks were worn during the procedure. The patella was extracted from the knee joint using sterile forceps and a no.22 scalpel blade (Feather, USA #72044-22) to detach ligaments from the bone. A sterile single edged industrial razor blade (VWR Scientific, USA #55411-005) was used to cut the remaining connective tissue. Once removed from the joint, the patella was irrigated with Dulbecco's Phosphate Buffered Saline (Sigma, USA #D-8862) at room temperature using a sterile plastic squirt bottle to eliminate any surface particles. The articular cartilage surface was inspected for qualitative evidence of cartilage damage. Only healthy, non-arthritic patellae were used. This included patellae that showed no signs of fibrillation or other signs of cartilage degeneration. Patellae with visual signs of degeneration were excluded from the study. Bottles of 500 ml PBS with 10 ml Penicillin and Streptomycin (Sigma, USA #P-4333) were previously prepared and patellae were placed in a beaker filled with this solution at room temperature until ready for potting in the Poly Methyl Methacrylate (PMMA) mold. Spherically bottomed PMMA molds were created to hold the patellae securely during impaction, as shown in Figure 9.



Figure 9. Patella in PMMA Mold

Fresh sterile sheets were placed on the counter in preparation for patella extraction from the corresponding left knee. The above steps were repeated for a left knee. Immediately after patella extraction, PMMA mixtures were prepared (to create individual molds for each patella) using 80g sterile PMMA powder and 40cc sterile PMMA (Osteobond Copolymer Bone Cement, Zimmer, Inc., USA #1101-08) liquid at room temperature. The bony non-articular surface was pressed into the partially set PMMA in the spherically bottomed mold to create an imprint. The patella was immediately removed to prevent any heat related damage. When the PMMA was completely set, the patella was placed in the cement (Figure 9).

### **7.3 *In vitro* Patella Impactions**

Sterile sheets were placed over the sterile stainless steel spherically bottomed holder of the MTS Mini Bionix II hydraulic load frame (MTS Corp., Minneapolis MN, USA). The PMMA-embedded patella was secured, cartilage side up in the spherical steel holder with the matching spherical cavity that allowed the patellae to be rotated so that the articular surface

of each facet could be aligned perpendicular to the impactor. The stainless steel, non-porous, cylindrical impactor was 10 mm in diameter and 7.7 mm wide. The impactor, in series with a three degree of freedom piezoelectric load cell, created a uniform plane strain loading along the 7.7mm length of the impactor (Figure 10). The piezoelectric load cell measured force in three directions: radial shear, longitudinal shear and axial force.

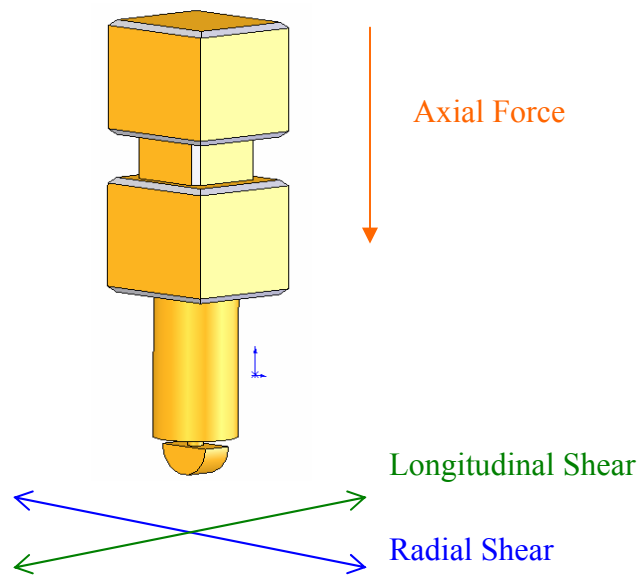


Figure 10. Piezoelectric Load Cell. Measurement of force in three directions in series with the contoured impactor.

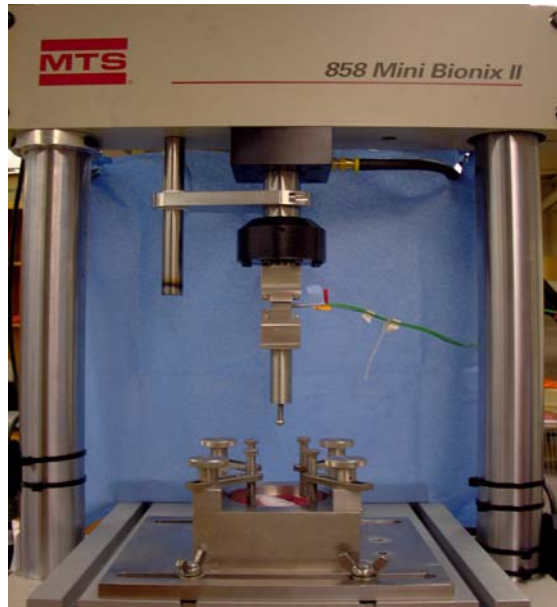


Figure 11. The MTS Mini Bionix Hydraulic Load Frame

The normal or axial force was also recorded by the MTS (Figure 11). The patella was rotated on the x-y positioning jig to align the facets as needed. Patellae were kept moist during the procedure by spraying them periodically with sterile PBS. To create reference markers for the center of impaction during histological analysis, patellae were marked prior to impaction with green-colored tissue marking dye (Polysciences, Inc. USA #24110) that was previously filtered with a sterile syringe filter. The dye was applied using a sterile wooden applicator stick. One dot was placed on each end of the impaction site which acted as a landmark to allow for repeatable location of the impaction site (Figure 12).



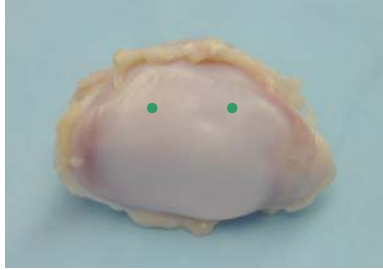


Figure 12. Location of Tissue Dye Marks (on one facet).

Controlled mechanical injuries were produced on each facet at a displacement rate of 25 mm/sec using the MTS load frame, to pre-selected force levels of 1000 N (moderate) and 2000 N (high). These force levels were chosen to obtain certain levels of gross tissue damage and they are similar to those previously found to be associated with cell death and matrix changes associated with impact loading.<sup>44,59</sup> Non-impacted patellae were used for controls. Control patellae (which were also marked with tissue dye in the same general area as the impacted specimens) allowed for comparison of changes with those resulting from the impact injury.

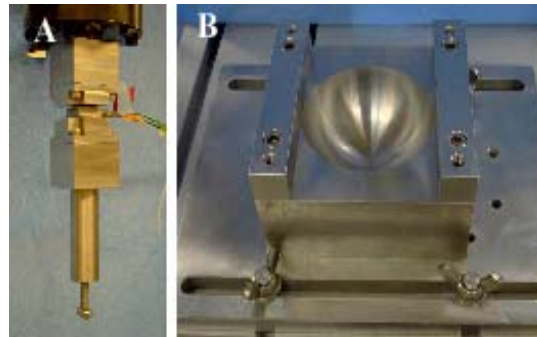


Figure 13. Impactation Apparatus A. Impactor and three-degree of freedom piezo electric load cell B. Holder for potted patellae.

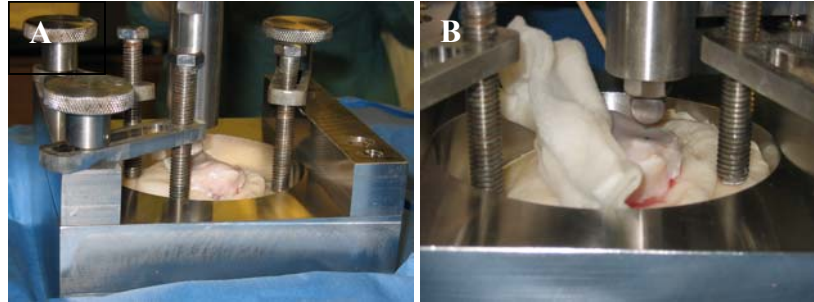


Figure 14. Patella in Impaction Apparatus. A. Patella secured or impaction B. Impactor near patella surface.

Using the MTS machine (Figures 11, 13 and 14), patellae were impacted twice, once on the middle of each facet, which provided two sites for analysis. Cartilage from medial facets was used for cell viability and proteoglycan analysis in this study. Cartilage from lateral facets is intended for future research involving biochemical analyses.

#### **7.4 Patella Organ Culture**

Following impaction, patellae were separated from their PMMA molds. Using 400ml plastic beakers, each patella was rinsed three times and then irrigated using a sterile plastic squirt bottle with PBS and antibiotics (penn. 100 units/ml and strep. 100 $\mu$ g/ml). Using sterile techniques under a laminar flow hood, entire patellae were placed in 100x80 mm Pyrex dishes, secured in a sterile stainless steel wire holders. These wire holders were custom built to position the patella cartilage side up in the center of the dish. Enough culture media (approximately 280 ml) was provided to completely immerse the patellae (Figure 15). Culturing intact patellae avoids the risk of materials escaping from cut tissue or the exposed marrow cavity from affecting the cartilage tissue while in culture. Each bottle of culture media consisted of 500ml Dulbecco's MEM/Ham's F-12 (Sigma, USA #D8437) with 50ml of 10% Fetal Bovine Serum (Sigma, USA #F2442), 12.5 mg L-Ascorbic Acid 2-Phosphate (Sigma, USA #A8960) and 5ml Penicillin-Streptomycin (Sigma, USA #P-4333). Media

was changed daily under a laminar flow hood using a 5 ml sterile pipet and an aspirator to remove the old media. Fresh media at room temperature was then poured in the glass dish, careful not to let the media bottle come in contact with the glass. Specimens were then maintained at 37°C in a CO<sub>2</sub> water-jacketed humidified incubator (Fischer Scientific) with 5% CO<sub>2</sub>.

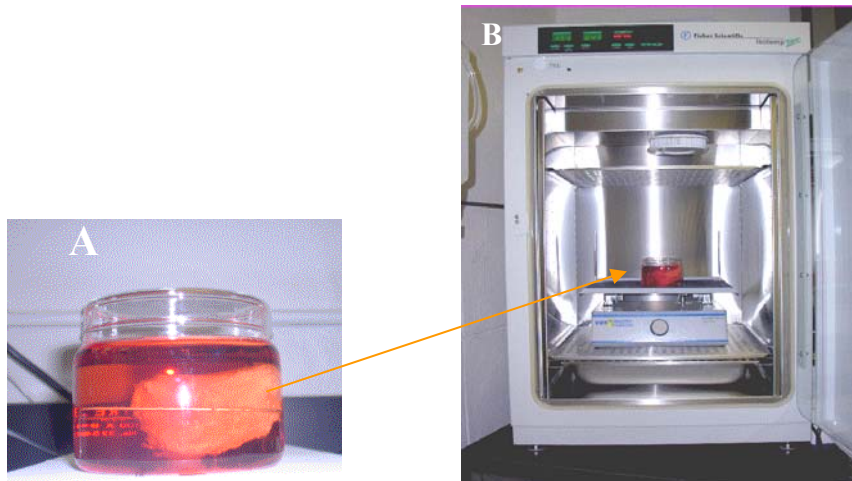


Figure 15. Patella Incubation, A. Patella in media, cradled in stainless steel wire holder B. Patella in incubator.

Culture dishes were kept on a rocking platform in the incubator to constantly stir the media, ensuring that its contents were evenly distributed. Patellae remained in culture for 0, 3, 7 or 14 days to allow the subsequent degenerative changes to be followed. All specimens were extracted, impacted and put in culture within 3-4 hrs of animal sacrifice.

### 7.5 Tissue Analysis

After removal of patellae from culture, entire medial facets (with the subchondral bone attached) were cut out using a band saw and placed in PBS prior to cell viability staining in an MTT (3-[4,5-dimethylthiazol-2-yl]-2,5-diphenyltetrazolium bromide) Thiazolyl Blue

assay (Sigma, USA #M5655). The MTT assay uses a tetrazonium salt that is converted by mitochondrial dehydrogenases in viable cells to an insoluble product termed purple formazon, which gives the viable cells an indigo color.<sup>16,57</sup> A non-sterile stock solution consisting of 20 mg Thiozoly Blue and 4ml Dulbecco's Modified Eagle's Medium: F-12, without phenol red (Sigma, USA #D6434), per (medial) facet was prepared. Next, 4 ml per facet of this stock solution and 36ml of the above DMEM Ham's F-12 was put in a 150 ml beaker. The now non-sterile facets were immersed in beakers of MTT solution with the cartilage surface facing up. The container was sealed with parafilm and placed overnight in an incubator at 37° C. After 24 hours, facets were rinsed three times with PBS and fixed in formalin for at least 24hrs to prevent matrix elements from escaping the tissue. After fixation, digital pictures of the facets were taken and rectangular cartilage sections (approximately 8X15mm) were separated from the subchondral bone of each facet using a scalpel. Each section was then immersed for 24 hours each in increasing concentrations of 60%, 80% and 90% Tissue-Tek OCT Compound (VWR Scientific, USA #25608-930) with PBS respectively. The center of impaction was re-marked with yellow tissue marking dye (Polysciences, Inc. USA #24112) in order for better visibility against the indigo-colored MTT stain. A line was drawn between the dots which allowed for repeatable location of the center of impaction on histology sections (Figure 16A). When ready for freezing, cartilage sections were cut in half through the center of impaction and perpendicular to the tissue dye line. The two halves were placed in a Tissue-Tek Cryomold (VWR Scientific, USA #4557). The mold was filled with OCT compound with the cut surfaces up against the edge of the mold for easy access to the desired tissue area during the cryocutting process (Figure 16B).

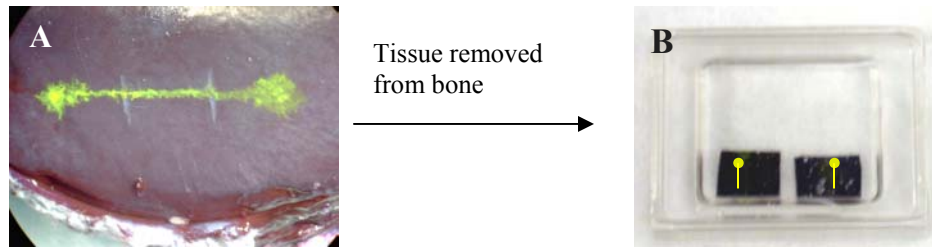


Figure 16. Tissue Preparation and Freezing, A. Medial facet, stained with MTT and the impact center re-marked with tissue dye. B. Cartilage sections cut through impact center and mounted in OCT gel.

Specimens were frozen in the gel using dry ice pellets in 100% Ethanol. Frozen tissue samples were labeled and stored in a freezer at  $-80^{\circ}\text{C}$  until ready to be cryocut and counter-stained with Safranin-O. Safranin-O is a cationic dye that binds stoichiometrically to the fixed negative charge content of GAGS (i.e. chondroitin-6-sulphate) in the articular cartilage matrix.<sup>27,51</sup> Cryosections of  $6\ \mu\text{m}$  thickness were cut using a Leitz cryostat. Sections intended for cell viability quantification were counter-stained with 0.01% Safranin-O aqueous solution for 10 seconds, resulting in a light pink colored extracellular matrix. Sections intended for proteoglycan distribution analyses were stained with 0.1% Safranin-O aqueous solution for 1 minute, resulting in a dark pink or red colored matrix. Sections were then put on microscope slides that were precoated with a mounting medium of glycerin jelly for lightly stained Safranin-O sections and Permount (Fisher Scientific) for darkly stained Safranin-O sections.

## 7.6 Data Collection

Preliminary tests using ultra low load Fuji film on separate test patella were used to calculate the contact radius of the impaction. Half of the total width of the contact area was used as the impact radius. Calculations determined that a value of 1640 (or 1.64 mm from the center of impaction) corresponded to the contact radius ( $r$ ), for a medium impaction at 40X

magnification. An average value of 1790 or (1.70mm from the center of impaction) corresponded to the radius (r) of a high impaction. Therefore these values were used to determine the metric distance of  $\pm 2r$ ,  $\pm r$  and  $\pm r/2$  from the impact radius, “0” (Table 4 and Figure 17). For example, radial position  $2r$  was approximately twice the contact radius ( r ) and position  $r/2$  was half the contact radius, and so on. Since the radii for moderate impactions were smaller, these were used to analyze control patellae.

Table 4. Distances From Impaction Center (in millimeters), calculated from the position of the contact radius at 40X magnification.

	<b>-2r</b>	<b>-r</b>	<b>-r/2</b>	<b>0</b>	<b>+r/2</b>	<b>+r</b>	<b>+2r</b>
<b>Controls, Mediums (mm)</b>	-3.28	-1.64	-0.82	0	0.82	1.64	3.28
<b>Highs (mm)</b>	-3.58	-1.79	-0.89	0	0.89	1.79	3.58

All histological sections were digitally captured by a high resolution Spot CCD color digital camera attached to a Nikon Y-FL research microscope under light microscopy. Images were saved in TIFF file format using a PC computer and quantified with Metamorph image analysis software. The tissue was divided into areas based on depth of the tissue and distance (i.e. radius) from the impaction (Figure 17B). In each of these areas the staining intensity and the number of dead cells, live cells, and total cells was measured.

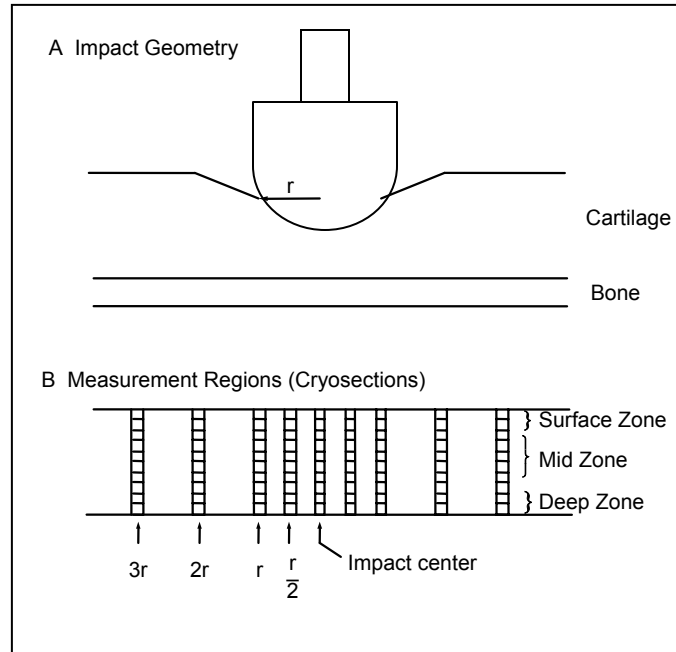


Figure 17. Impact Geometry, A. The contact radius ( $r$ ).  
 B. Location where the histology measurements were made.

Image analysis was performed using Metamorph imaging software with a 40X microscope objective. Starting at the center of impaction, pictures were taken at vertical displacements of  $173\ \mu\text{m}$  from the superficial zone to the deep zone. A journal was prepared in Metamorph to allow the microscope stage to move from the surface zone to the deep zone at the vertical increments of  $173\ \mu\text{m}$  in length. Each picture at these increments was  $220\ \mu\text{m}$  in width. When all pictures were taken from the center of impaction, a montage was created that stacked the individual pictures as a single column. The process was repeated at each radial distance to create one column each, creating 7 columns:  $-2r$ ,  $-r$ ,  $-r/2$ ,  $0$  (i.e. center of impaction),  $r/2$ ,  $r$ , and  $2r$  (Figure 18). The number of images per column ranged from 5 to 8, depending on the thickness of the tissue cross-section.

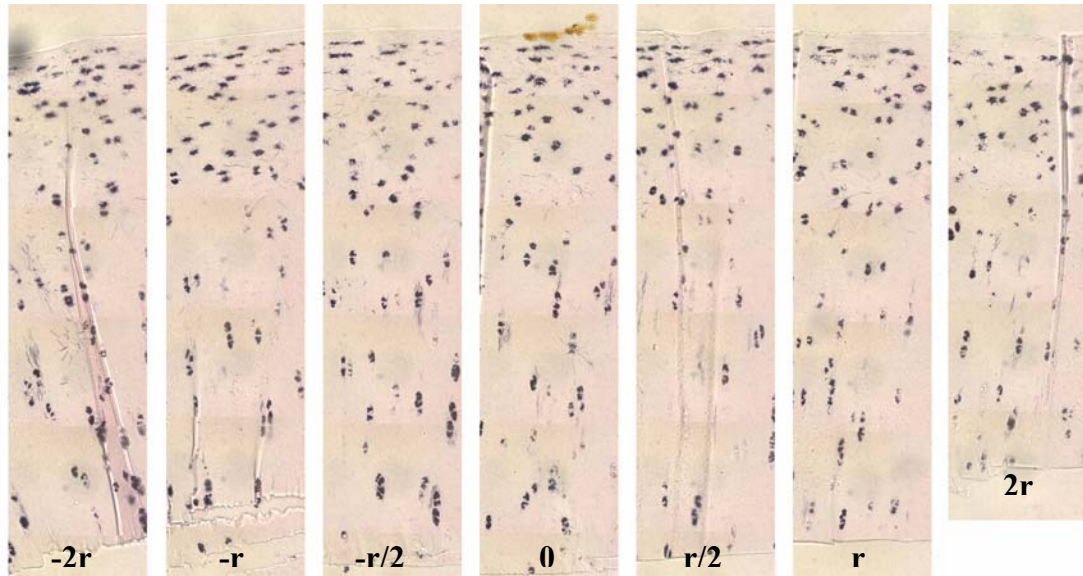


Figure 18. A Collective Montage. Seven montages (one for each radial position) for an MTT-stained specimen.

Each column was divided into 10 equal rectangular regions (Figure 19). The distribution of cell viability and proteoglycan concentration was examined through the thickness (i.e. depth) of each cartilage layer: 1-10. The area of the rectangles was influenced by the thickness of the cartilage. All slides were analyzed in random order with respect to force level, days in culture and date of impaction.



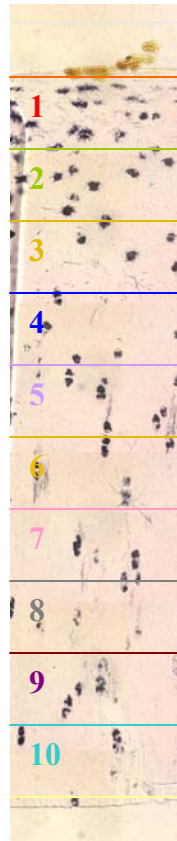


Figure 19. Tissue Column (divided into 10 regions for analysis).

### **7.7 Measurement of Safranin-O Staining Intensity: Proteoglycan Distribution**

Safranin-O staining was measured in each of the 10 regions. Stain intensity was quantified by measuring the pixel intensity of the stain in each region, with the intent to obtain an unbiased quantitative measurement of the proteoglycan distribution in a specific area. The pixel intensities, valued between 0-255, were used as a measure of proteoglycan distribution in each of the 10 regions. A value of 0 was most intense (i.e. black) and a value of 255 was least intense (i.e. white).

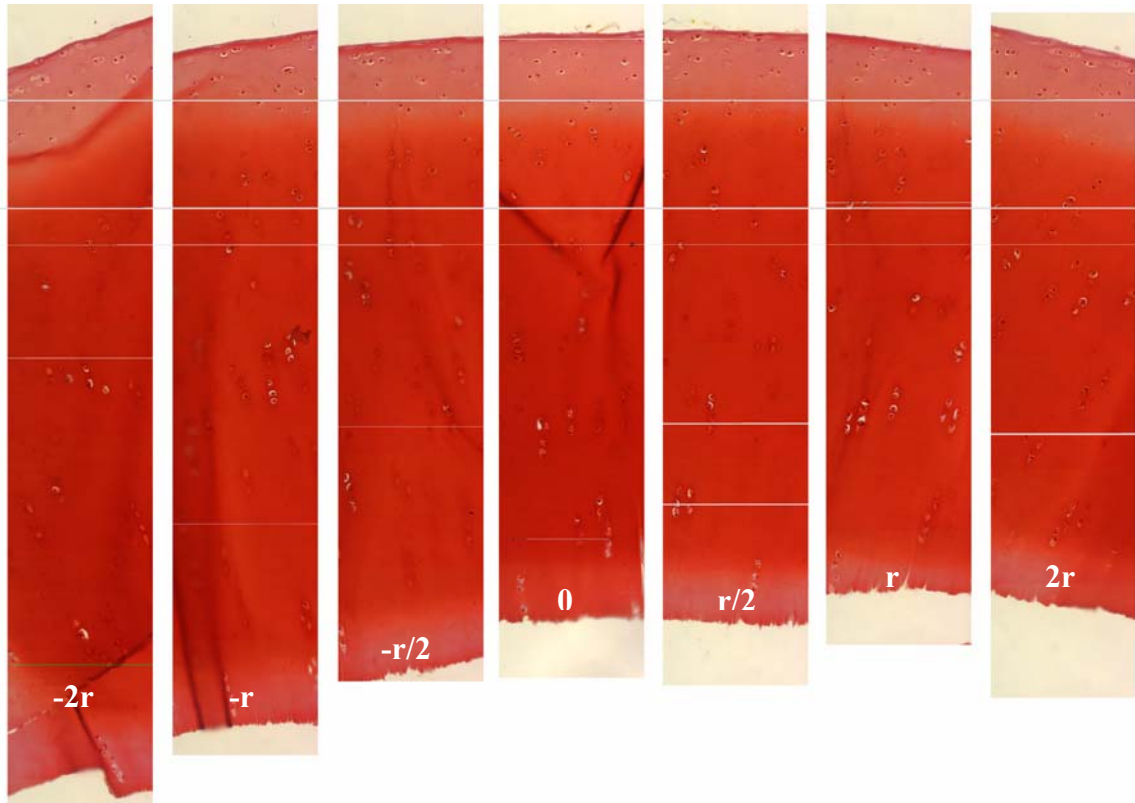


Figure 20. A Collective Montage. Seven columns (one for each radial position) for a control/normal specimen stained with Safranin-O.

To eliminate the intra-tissue variability, the average intensity at each region was then divided by the average intensity of the deep (region 10) at the center of impaction, in order to obtain a normalized intensity. These normalized values were used for the actual quantification of proteoglycan intensity. Measured intensity values ranged from 0-2, with 0 being darker and 2 being lighter than the intensity at depth 10 at the center of impaction. Regions of tissue with excessive tears, folding or abnormal coloration were excluded from the data set in order to avoid tainting the overall intensity calculations.

### 7.8 Quantification of Chondrocyte Viability

The number of live and dead chondrocytes was counted in each of the 10 regions. All cells containing any traces of indigo-colored MTT stain were designated as live. All

unstained cells were assumed to be dead. Cells were counted manually by labeling the live cells yellow and the dead cells green using Metamorph software. Cells at the borders of each region were counted only if they were more than halfway within the image region. The number of live and dead cells in each region was recorded manually into an Excel spreadsheet, along with the total number of cells in each region and total number of cells in the entire column (i.e. regions 1-10). Regions with 0 total cells or incomplete tissue sections were excluded from the data set. The regions with 0 total cells would have created a problem in determining the % dead cells because it would have been calculated in the spreadsheet as “0% dead cells” (i.e. 100% live cells), which was not the case in these regions. Abnormal cell death was classified as cells that may have died near the tissue edge, adjacent to the cut made with the band saw, when separating the 2 facets. The tissue sections near radial position  $\pm 2r$  were mostly affected by abnormal cell death. Incomplete tissue sections were those that could not fill the 220  $\mu\text{m}$  width at the edge of the histological section (i.e.  $2r$ ), therefore were not a complete section. Examples of these were specimens that were not cut wide enough to capture the entire array of radial positions.

## **7.9 Statistical Analysis**

The above collected data was logged into text files and exported to Microsoft Excel spreadsheets. Based on the balanced incomplete block design, an ANOVA was performed using SAS software to analyze the data using significance level of  $\alpha=0.05$ . Changes in Safranin-O staining intensity and the percent of dead cells were analyzed with the independent variables being impact level (control, medium, high), time in culture (0, 3, 7, 14 days), distance from center of impaction ( $r=0, \pm r/2, \pm r, \pm 2r$ ) and depth in tissue (levels 1-10).

Further analyses of specific comparisons within load-culture, load-depth, load-radial and radial depth interactions, were assessed using the pairwise Bonferroni criteria.

## **8 Results**

A total of 36 patellae (18 left and right pairs) were used in this study. Twelve patellae were impacted at the medium load level (with a target load of 1000 N), twelve for the high level (with a target load of 2000 N) and twelve were used for control. The actual loads obtained from the medium impactions were  $1047 \pm 122$  N normal,  $132 \pm 77$  N radial shear and  $48 \pm 29$  N longitudinal shear. The actual loads obtained from the high impactions were  $2239 \pm 178$  N normal,  $233 \pm 164$  N radial shear and  $81 \pm 61$  N longitudinal shear. Three patellae were used for each culture time for each of the three load cases. Two sets of analyses were performed to study the effect of impact stress on chondrocyte viability and proteoglycan content at 0, 3, 7 and 14 days after impaction.

### **8.1 Chondrocyte Viability**

The number of dead cells, live cells and total cells was counted and the percent of dead cells was assessed at each radial position and through the depth of the tissue. Overall analysis showed a significant load effect ( $p=0.002$ ), culture time effect ( $p= 0.005$ ), radial effect ( $p= 0.025$ ), and depth effect ( $p<0.0001$ ). There were significant load-culture and load-depth interactions but not significant load-radial, depth-radial or culture-radial interactions. The average percent of dead cells in the tissues for each load at all culture times were  $6.4 \pm 12.7$  % for the controls,  $19.5 \pm 21.2$  % for the medium and  $21.1 \pm 24.8$  % for the high impacted tissues, indicating an overall increase in cell death with increasing impact magnitude ( $p<0.0001$ ).

The medium and high impacted specimens both showed a significant increase in cell death after 3 and 7 days in culture compared to the unloaded controls ( $p < 0.0001$ ). However the difference between the medium and high impactations were only significant after 14 days in culture ( $p = 0.0006$ ), where the mean % cell death was  $15.59 \pm 17.69 \%$  for the medium load and  $22.01 \pm 22.92 \%$  for the high load. This indicated an overall higher percentage of cell death in the high impacted specimens than in the medium impacted specimens only after 14 days post-culture (Figure 21). For all loads and all culture times, there was an overall increase in the average cell death ( $p < 0.0001$ ) from  $3.13 \pm 6.97 \%$  (depth=2) to  $26.27 \pm 25.82 \%$  (depth=10). The top layer, depth 1, had significantly higher cell death ( $10.5 \pm 16.6 \%$ ) than depth 2 just beneath it ( $p = 0.005$ ).

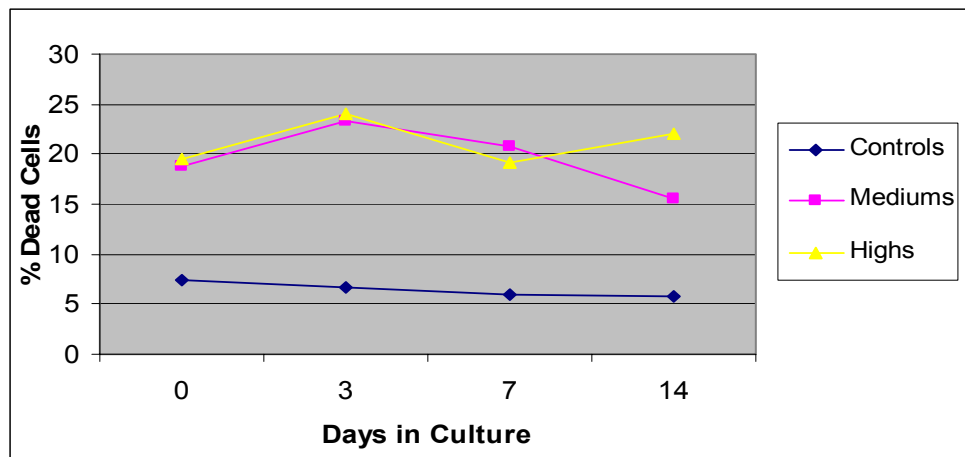


Figure 21. Mean Percentage of Dead Cells

At depth 7, the percent of dead cells in the high impact group at 0 days post-impact, was significantly higher ( $38.96 \pm 28.99\%$ ) compared to the controls ( $11.99 \pm 15.63 \%$ ) and mediums ( $17.91 \pm 24.75 \%$ ), where  $p = 0.043$ . For the high impactations after 3 days, the depths that showed a significant cell death increase compared to controls were 1-5 and 7-10 ( $p = 0.001$  to  $p = 0.042$ ). At the top layer (depth 1), the greatest increase in

dead cells in the high impacted specimens, compared to controls and mediums, was seen after 7 days in culture, increasing from  $7.4 \pm 14.6$  % at time zero to  $29.1 \pm 29.1$  % at seven days. At 0 days post impact there was also significantly more cell death for the medium impactations compared to controls within depths 1-2 ( $p=0.012$ ) and 9-10 ( $p<0.0001$ ). After 3 and 7 days in culture, there was generally a significant increase in cell death within depths 4-10 ( $p=0.003$  to  $0.016$  respectively) for the medium impacted specimens compared to controls. Therefore the percent of dead cells immediately after impactation (0 culture days) was greater in surface and in deep layers for the medium impactations and in the middle layers for the high impactations. Additionally, the cell death appeared only at the middle to deep layer for medium impacts after 3 days and at the surface layers and deep layer for high impacts after 3 days. In high impacted specimens at 14 culture days, the cell death then decreased to 32.9% and 32.2% at depths 9 and 10 respectively. The overall percentage of cell death after 7 and 14 days in culture was lower than the cell death at 3 days in culture ( $p<0.0001$ ). There were also a significantly greater number of total cells ( $p<0.0001$ ) and live cells ( $p<0.0001$ ) after 7 and 14 days in culture than at 0 and 3 days.

At almost all individual radial positions and load levels, the percentage of dead cells did not significantly change after 3, 7 and 14 days in culture compared to 0 days in culture.

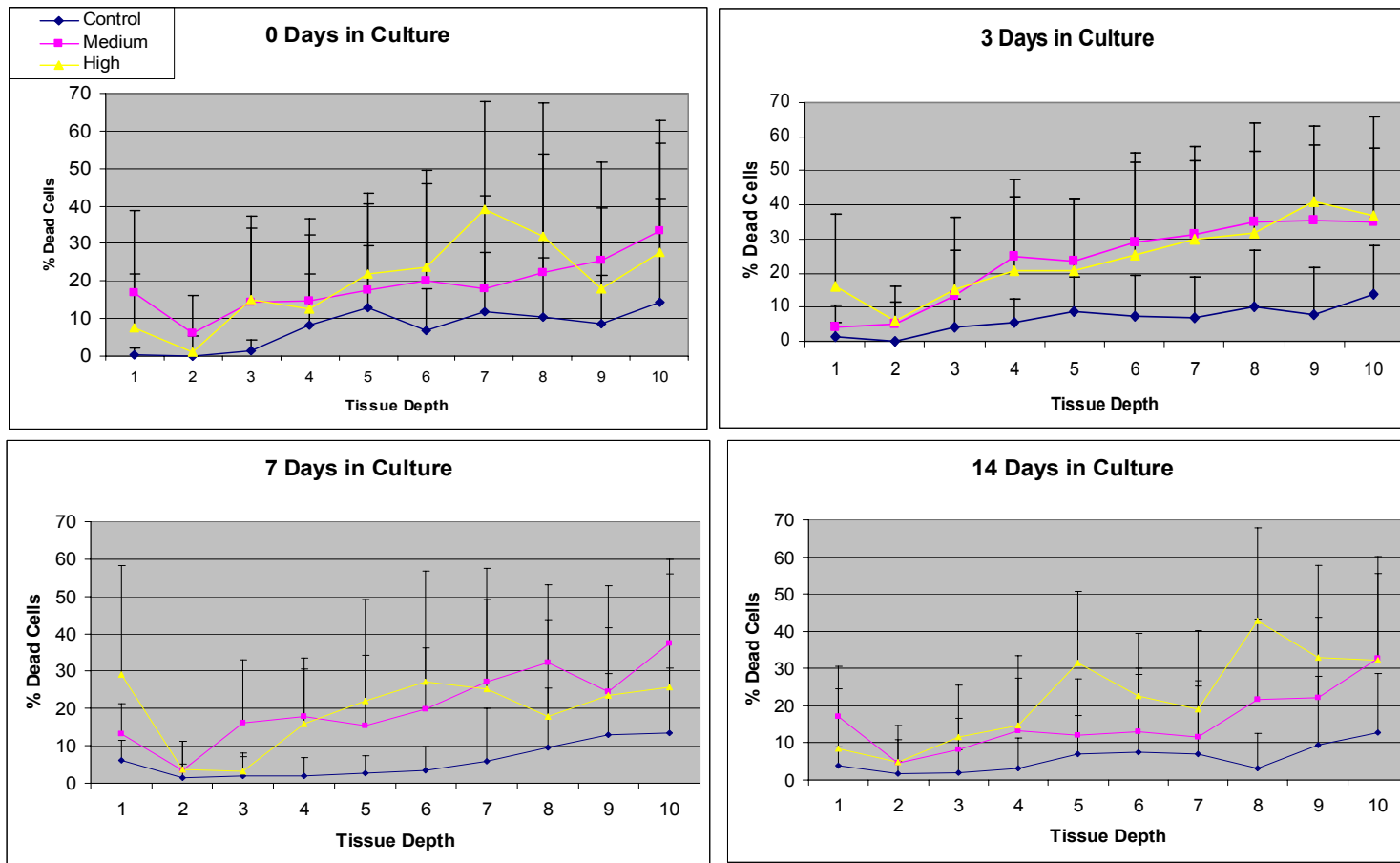


Figure 22. Percentage of Dead Cells by Tissue Depth - for all loads (control, medium, high) and culture times (0, 3, 7 and 14 days).

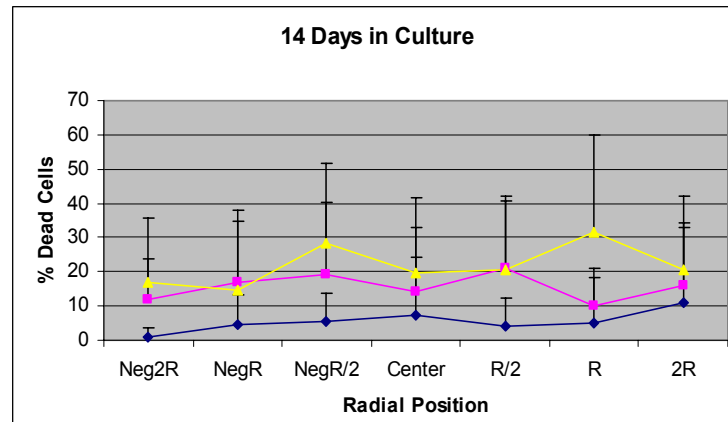
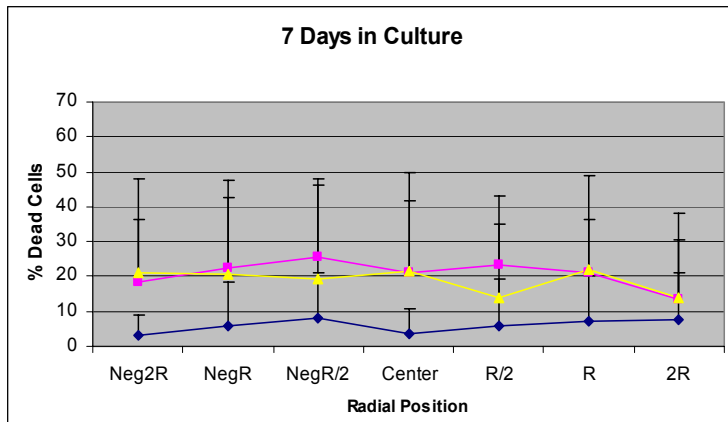
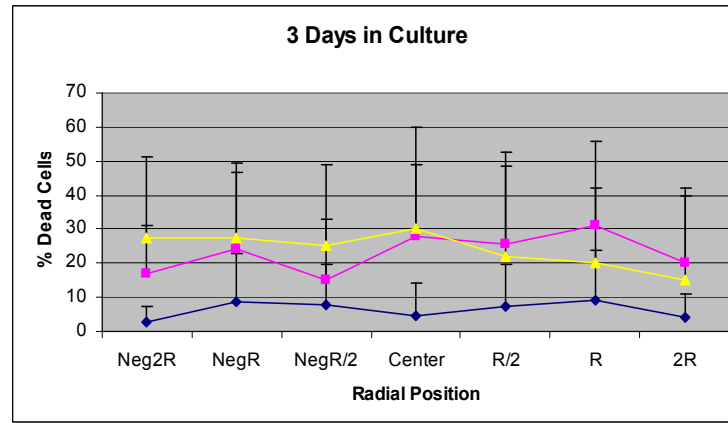
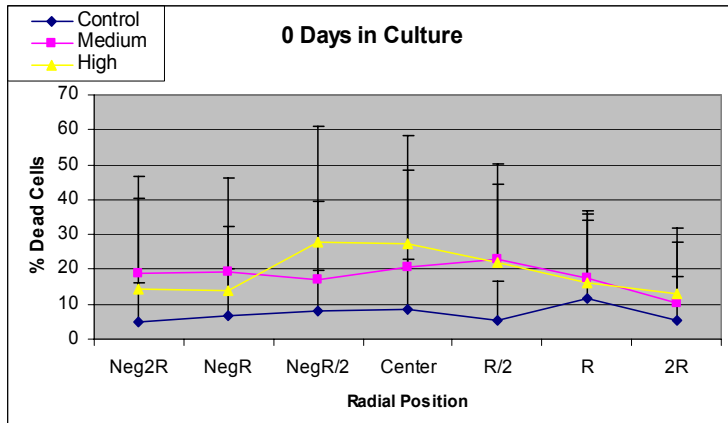


Figure 23. Percentage of Dead Cells by Radial Position - for all loads (control, medium, high) and culture times (0, 3, 7 and 14 days).



## 8.2 Proteoglycan Content

The proteoglycan content was assessed according to the color intensity and the normalized intensity (relative to the center position at depth 10), at each radial position and through the depth of the tissue. Overall analysis showed a significant load effect ( $p=0.002$ ), culture time effect ( $p<0.001$ ), radial effect ( $p<0.001$ ) and depth effect ( $p<0.001$ ). Interactions were significant for load-culture, load-depth and load-radial effects. The depth-radial interactions were not significant. For all depths 1-10, the normalized average intensities in the tissues were  $1.003 \pm 0.2$  for the control,  $1.04 \pm 0.2$  for the medium and  $0.97 \pm 0.3$  for the high impactions ( $p<0.0001$ ). This represented a trend of darker proteoglycan staining for the controls (relative to center position at depth 10) compared to the medium loads and darker staining for the high loads than controls. The normalized intensity values were significantly greater ( $p<0.0001$ ) in the surface layers (depths 1-2) and deep layers (depth10) than in the middle layers (3-9) for all specimens at all loads and culture times. For example, values were  $1.28 \pm 0.2$ ,  $0.95 \pm 0.2$ ,  $1.01 \pm 0.1$  for depths 1, 5 and 10 respectively. Similarly, all controls had lighter staining at the top and deep layers than in the middle layers ( $p<0.0001$ ), where values ranged from  $1.33 \pm 0.23$ ,  $0.922 \pm 0.91$ , and  $1.03 \pm 0.13$  for depths 1, 5 and 10 respectively, representing a higher concentration of proteoglycan in the middle layers than in the superficial and deep layers, which are consistent with the literature with respect to normal, untreated articular cartilage.<sup>40</sup> The normalized intensity differences within the tissues were only significant between depth 1 compared to depth 10 (at the center of impaction) for the control and medium ( $p=0.002$ ), and not significant for the high loaded specimens. For example, PG concentration at the top layer of the control and

medium loaded specimens was significantly lighter than depth 10 at the center of impaction (Figure 24).

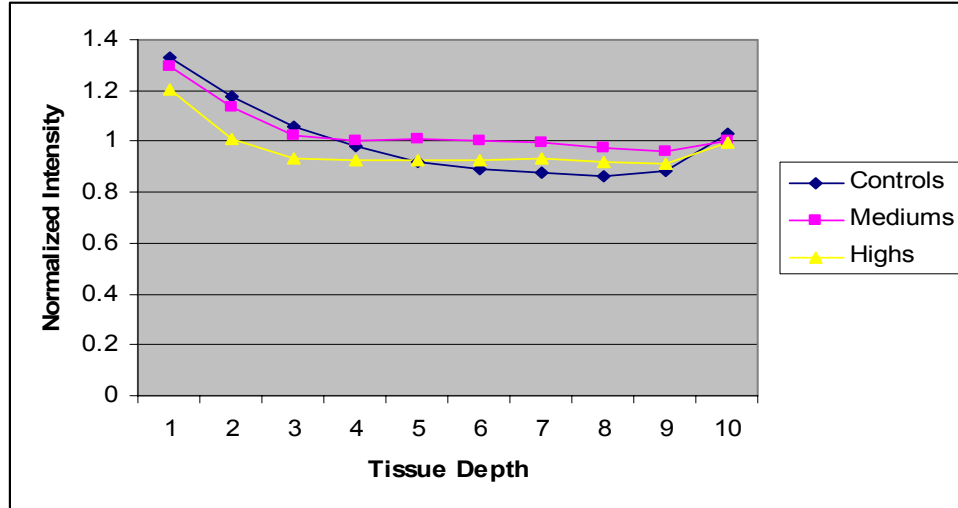


Figure 24. Mean Normalized Intensity by Tissue Depth - for each load level.

At 0 culture days, the normalized intensity values were  $0.90 \pm 0.2$ ,  $1.01 \pm 0.2$ , and  $1.17 \pm 0.3$  for the control, medium and high load levels respectively ( $p < 0.0001$ ). An opposite effect was seen after 7 and 14 days as the PG concentration became higher for the medium impact specimens ( $1.16 \pm 0.22$  and  $1.03 \pm 0.15$ ), than the high impacted specimens ( $0.92 \pm 0.14$  and  $0.88 \pm 0.23$ ). For each load level and corresponding culture time, the only significant change in PG concentration was seen at depth 1 for the medium impacted specimens after 14 days ( $p = 0.002$ ).

There were no differences in normalized intensity between radial positions for medium impactations. At day 0 for the high impactations, radial positions  $-2r$ ,  $-r$  and  $-r/2$ , had lighter safranin-O staining compared to the other radial positions ( $0$ ,  $+r/2$ ,  $+r$  and  $+2r$ ) at this load and culture time, indicating a lower proteoglycan content in the negative

radial positions than in the positive positions ( $p=0.0003$  to  $0.02$ ). This was due to an atypical piezo-radial shear force for specimen 'H0RMax\_9.12.03' where the shear force was  $447.05$  N, which was twice the average values obtained for the radial shear forces of high impactations. After 3-7 days in culture, there were no more significant differences between radial positions for the high impacted specimens.

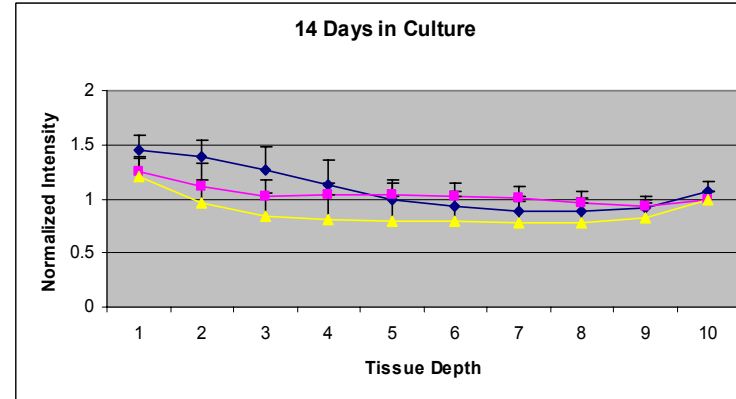
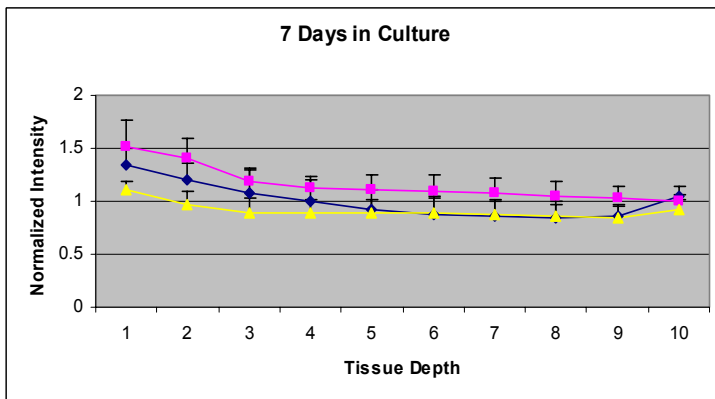
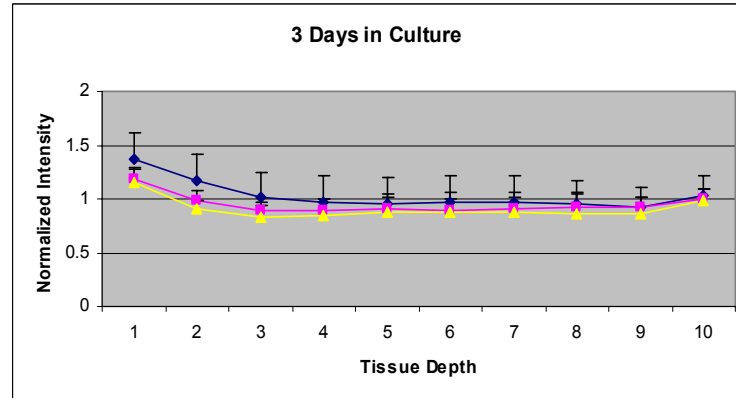
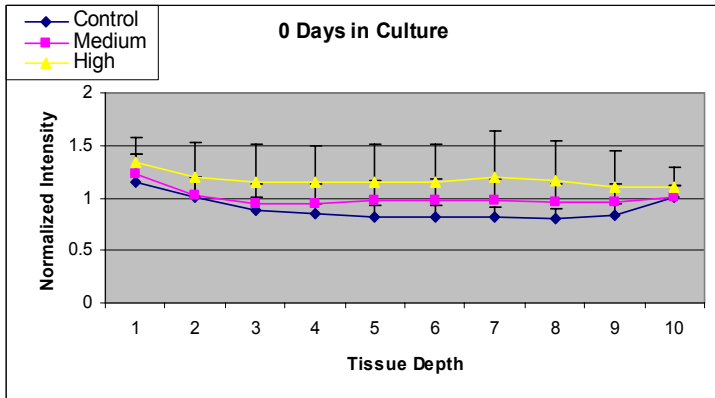


Figure 25. Normalized Intensity by Tissue Depth - for all loads (control, medium, high) and culture times (0, 3, 7 and 14 days).

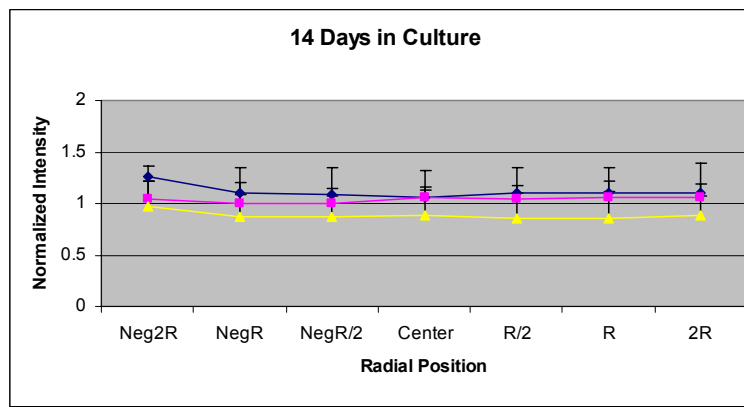
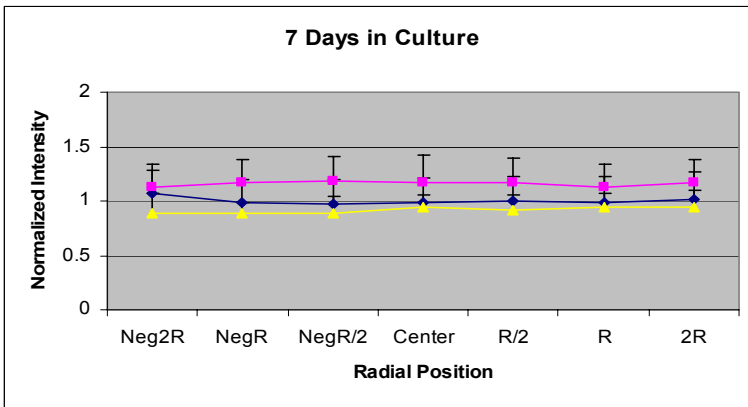
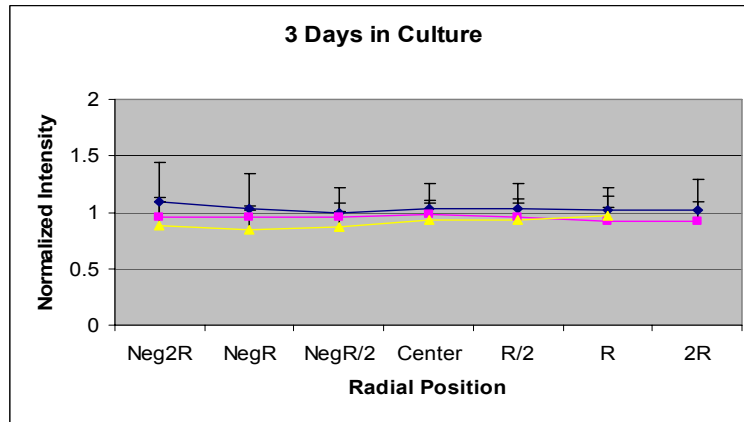
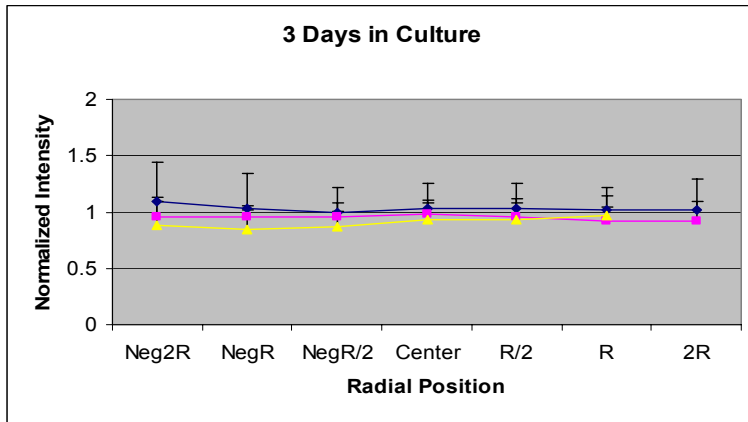


Figure 26. Normalized Intensity by Radial Position - for all loads (control, medium, high) and culture times (0, 3, 7 and 14 days).

## 9 Discussion

The main objective of this study was to evaluate articular cartilage cell viability and changes in proteoglycan content caused by impacts of different force levels at various culture times after the impact. Several studies have shown that impact injuries on articular cartilage can lead to cell and matrix changes similar to those seen in the degenerative process that leads to osteoarthritis.<sup>5,9,13,17,25,28,31,45,55,56,59</sup> However there are conflicting results and it is still unclear if matrix changes are cell-mediated or caused by direct damage. No known studies have examined both the time and location-specific effects of impact loads on intact (patella) specimens for up to two weeks in culture. The outcome of such test criteria in this study is one step in understanding the early degenerative changes that can lead to osteoarthritis.

The findings in this study showed more significant correlations between load and culture time in comparison to tissue depth, than between load and culture time in comparison to radial position from the impact center. Tissue sections excluded from the data set, due to irregularities, reduced the power of statistical analysis. Most excluded sections were from radial sections -2r and +2r, and may be partially responsible for the lack of significance of radial effects. For example, at least 1 section (from -2r and/or +2r) of specimens: C0, C3, C14, M3, H7 and H14 was eliminated from the cell count data set. At least 1 section (from -2r and/or +2r) of specimens: C3, C14, M0, M3, H0, H3, H7 and H14 was eliminated from the proteoglycan data set. In addition, values obtained for normalized intensities were calculated relative to each specimen's own depth=10 at the center of impaction. This could pose a problem when examining the staining changes between tissues, since the staining is relative to the deepest (depth = 10) center region.

Therefore significant comparisons could only be made within tissues (and not between impacted tissues or between impacted and un-impacted tissues). Comparisons made between impacted tissues or between impacted and un-impacted specimens were only trends, and not necessarily significant. One way to reduce this problem would be to calculate normalized intensity for each depth in relation to the corresponding depth in the tissue column at the center of impaction. For example, use depth 1 at the center to calculate the normalized intensity for depth 1 at radial position  $2r$ , and so on. However this method is very complex and may promote further confusion. Therefore another way would be to develop standards for proteoglycan concentration that could be used to compare staining obtained from experiments. If the  $\pm 2r$  sections were not problematic, these sections would have been better to use for normalized calculations since the tissue at these positions were expected to be normal.

In agreement with the first statement in the hypotheses, it was found that the cellular and PG changes depended on the magnitude of impact load and time in culture. Findings indicated that the average percent of dead cells (regardless of culture time) increased with increasing impact load. Regardless of the time in culture, the normalized PG concentration overall was lower in cartilage exposed to medium impactions than in high impacted specimens. The depth-dependent changes in cell viability and proteoglycan content however, depended on both impact magnitude and the length of time that the tissue was in culture.

In summary, high impactions induced initial cell death in the middle layer which then spread to the superficial and deep layers with increasing culture time. This result was opposite to what was predicted in the hypothesis. Despite an initial decrease in PG

concentration (immediately after the high impactation), PG content steadily increased from the surface and deep layers to the middle layers as culture time increased. Again, it should be noted that these values were compared to normalized intensities in control tissue, and are not necessarily statistically significant. Nonetheless, studies have reported similar results where proteoglycan biosynthesis decreased (and water content increased) with increasing impact stress within the first 24 hours.<sup>5,13,55</sup> Another study by Ewers *et al.*,<sup>18</sup> found that after initial GAG loss from cartilage subjected to high loading rates after 1 day, the GAG loss decreased after 2-4 days. The current study shows evidence of a relative increase in PG content in areas that contain significant cell death. However the mechanism for the trend of higher levels of PG content in the high impacted specimens compared to the mediums still needs further investigation. The difficulty in comparing control PG levels with impacted specimens is, again, attributed to the method of calculating normalized intensity. Once a valid method of normalized intensity calculations is established however, it would be interesting to investigate the effect of impact loads on the collagen matrix and to measure water content in association with PG content and cell viability, since the collagen fibrils are responsible for anchoring the proteoglycans and preventing them from expanding.

Secondly, the findings for medium impactations were not as linear as the high impacted specimens and involved more fluctuation in terms of PG concentration levels. Medium impactations induced initial cell death in the surface and deep layers and the presence of cell death continued to occur mostly in the middle to deep layers with increasing time in culture. This study showed that in medium impacted specimens, cells were alive in areas of increased PG content and cells were dead in areas where PG



decreased. Similarly, a study that used identical load magnitudes suggested that this result may have been caused by the cell death in areas of low PG content, resulting in a cell-mediated degradation of proteoglycans.<sup>18</sup> This result may have also been due to a cellular response due to matrix injury including increased rates of matrix turnover and remodeling. On the other hand, it may have reflected an increased passive loss of proteoglycan due to mechanical disruption of the matrix.<sup>44</sup> In the current study, since the PG content increased and finally decreased again (significantly in the top layer), compared to depth 10 at the impact center for medium impactations throughout the time in culture, this may have been due to intrinsic remodeling of the cartilage matrix which can also occur without any external signs of degeneration. Investigators have reported that if the damage is minimal, complete surface repair may result.<sup>56</sup> Therefore in the case of the higher proteoglycan content in the high impacted cartilage in the current study, it is unlikely that this increase is due to repair and should probably be attributed to alternate mechanisms. Further study is necessary to identify and investigate these mechanisms.

Interestingly, 7-14 days after impactation, the overall cell death decreased and there was also a significant increase in the total cells. The decrease in the percent of dead cells after 7 days post-impactation may have been a result of the dead cells being more difficult to recognize against the surrounding extracellular matrix due to physical damage to the cell (and its membrane, nucleus and/or cytoskeleton) via its attachments to the pericellular matrix.<sup>55</sup> Apoptotic cells have been reported to be shrunken in appearance with blebbing of the cell membrane into smaller apoptotic bodies, condensation of the cytoplasm and nucleus, and absence of the pericellular matrix.<sup>9,24,41</sup> A study conducted by D'Lima *et.al.*,<sup>13</sup> reported a progressive increase in the percentage of apoptotic

chondrocytes from 6 hours to 7 days post-injury. Another study by Triantafillopoulos *et.al.*,<sup>56</sup> found a combination of necrotic and apoptotic-like cell morphology after an impact injury. At 8 days after injury most chondrocytes had a well-organized nucleus but the cytoplasm and cytoplasmic membrane were completely disorganized. At 15 days post-injury, there was a total disorganisation of the nucleus, aggregation of lacunae in the cytoplasm some traces of the cytoplasmic membrane. Since the cell viability assay used in the current study did not stain the dead cells, the unstained cells displaying the above mentioned characteristics, especially after 7 days post-impaction, may have been difficult to see even at 40X magnification and were therefore not counted (Figure 27). If these unstained cells were not counted due to apoptotic-like morphology, it is possible that some of the cell death occurring after 7 and 14 days after impaction died via the apoptotic pathway. If this was the case, most of the dead cells at 0 and 14 days may be result of necrosis.



Figure 27. Live (MTT stained) and Dead Chondrocytes. Arrows indicate dead cells.

In a study that performed cyclic impacts on cartilage explants, Chen *et.al.*,<sup>9</sup> found that 32% of dead cells after the first 2 hours post-impaction were characteristic of

necrosis. After 2 days the proportion of cells positive for apoptosis was 73%, concluding that necrosis occurred before apoptosis in repeated cartilage impacts. However future analysis involving apoptosis and necrosis specific cell assays using single impact protocols are necessary to support this theory.

The overall increase in total cells with increasing culture time may have been a result of cellular proliferation. Many studies have shown that there is evidence of proliferative activity in OA chondrocytes resulting in chondrocyte clusters typical of OA cartilage.<sup>2,30,54,56</sup> In experimentally wounded cartilage explants, Tew *et.al.*,<sup>54</sup> observed proliferation in the surface region at 5 days post-injury, although it declined to nonsignificant levels by day 10. This proliferative effect may have also been partly responsible for the decrease in percentage of cell death after 7 days post-impaction in the current study.

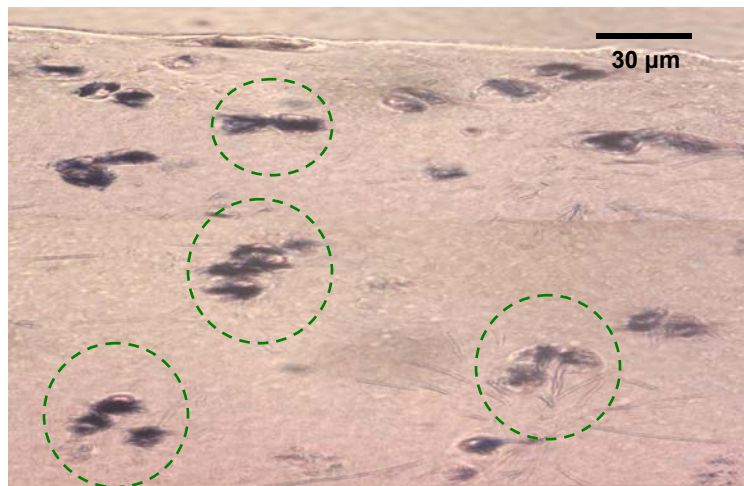


Figure 28. Cell Clusters. Observed in the surface zone (indicated by circles) of a high impacted specimen, 'H14LMax\_8.12.03'.

As shown in Figure 28, evidence of cell clusters (groups of 2 to 6 closely-associated cells) was observed in both 7 and 14 day specimens but were not accounted for in the

data set. The chances of proliferation contributing to tissue repair are low however, since the cell clusters do not necessarily contribute to matrix anabolism.<sup>1</sup>

Generally speaking, articular cartilage subjected to medium (1000 N) impact forces produce cell death initially at the surface and deep layers, proceeding to the middle layers with increasing time in culture. The overall lower proteoglycan content for medium (1000 N) impactations may be a result of cell-mediated matrix degradation. Articular cartilage subjected to high (2000 N) impact forces had cell death initially at the middle layers, proceeding to the surface and deep layers with increasing culture time. The overall higher proteoglycan content for high impactations may be the cause of cell death due to matrix injury. However further study is needed to examine these load dependent cellular and matrix interactions. Improvement is also needed on the method of normalized intensity calculations, in order to make comparisons between tissues and not just within tissues. The non-significant differences in radial position for both the cell and PG data may have been due to the size and shape of the impactor. An impactor with a smaller surface area (i.e. pointier) would have created a more concentrated load, thus creating the potential for more significant load effects.

The results of this study indicated that the magnitude of an impact load can significantly affect the degree of matrix changes throughout the depth of articular cartilage tissue over time. These findings suggest an interaction between cell death and proteoglycan content in this process. However a larger sample size would be necessary to confirm these findings. Future studies will determine the specific mode of cell death and the role of other articular cartilage components in the degenerative pathway leading to osteoarthritis.

## **10 Recommendation for Future Research**

### **10.1 Stain for General Cell Death, Apoptotic Cell Death and Cell Proliferation**

One challenge of this research was determining whether the decrease in dead cells after 7 to 14 days post-impact was due to some (unstained) dead cells being less visible against the matrix and may not have been counted. If this problem could be eliminated, the true number of dead cells could be quantified and the outcome of the experiment may change. Most stains for general cell death are immunofluorescent probes and require fluorescent microscopy to be seen. For the continuation of this study it would be ideal to administer a stain that is specific for cell death and to use this stain together with the viable cell assay, MTT, in order to see all cells using light microscopy.

It is also possible that some cells that were counted as alive were in the process of dying via apoptosis. In order to determine if these cells are dying by this process, it is necessary to use the TUNEL stain to label the apoptotic cells. Other cells that were counted as live may have been a product of proliferation. An *in vitro* label, such as <sup>3</sup>H-thymidine can detect cell proliferation.<sup>54</sup> Also, the “nearest neighbor” method can be used to measure the distance between cells over time (in addition to counting individual cell clusters).

### **10.2 Damaged Type II Collagen Analysis**

In order to determine the role of type II collagen in cartilage matrix degradation, an antibody that recognizes epitopes available for binding denatured, but not native type II collagen such as COL2-3/4m can be used.<sup>54</sup> The detection of the damaged type II collagen could either be in the form of a tissue stain or detected from retrieved culture media. Observing the changes in type II collagen may aid in understanding matrix

degradation in correlation with depth-dependent changes in cell viability and proteoglycan content after an impact injury.

### **10.3 Assessment of Tissue Fibrillation and Subchondral Bone Damage**

The depth-dependent behavior of articular chondrocytes may vary with the presence or absence of subchondral bone damage. Also, fibrillation or cracks in the tissue may also affect the distribution of chondrocyte death and proteoglycan concentration changes, depending on the extent of fibrillation. Tissue fibrillation was not observed in this study, perhaps due to load magnitudes not being high enough. Future experiments (using a greater number of specimens) involving observations of both the bone and cartilage layers may determine the magnitude of impaction necessary to create fibrillation and subchondral bone damage in addition to where such damage is located in relation to the center of impaction. Several studies have used chelating agents such as calcein, alizarin complexone and tetracycline, which label  $\text{Ca}^{2+}$  ions exposed on the surfaces of microcracks.<sup>33</sup>

### **10.4 Effect of Axial Load on Chondrocyte Shape and Volume**

This study examined the effect of an axial impact load on chondrocytes in general. Few studies have determined the effect of such a compressive load on individual chondrocytes, but attention to this area of research is growing. Since a chondrocyte has the ability to use mechanical signals to regulate its metabolic activity,<sup>21</sup> it is necessary to characterize its behavior under physiological loading to determine its role in matrix metabolism. One way to do this would be to design a device large enough to accommodate the cartilage specimen and its compression tool, but small enough to fit under a microscope to be viewed with at least a 40X magnification. The compression tool would

need to be accommodated by a measurement apparatus adequate for such a small device, such as a strain gage to measure the applied force. In addition, an optimal cell viability assay would be needed to view the individual cells and their corresponding membranes. Previous experiments have used CMFDA (cell tracker green) for live cell labeling and ethidium homodimer to label dead cells. These experiments can determine the effect of an axial load on a chondrocyte's shape, volume and potentially its metabolic activity and gene expression during compression.

## References

1. Aigner, T. and Kim, H.A.(2002). "Apoptosis and cellular vitality." Arthritis & Rheumatism **46**(8): 1986-1996.
2. Aigner, T., Hemmel, M., Neureiter, D., Gebhard, P.M., Zeiler, G., Kirchner, T. McKenna, L.(2001). "Apoptotic cell death is not a widespread phenomenon in normal aging and osteoarthritic human articular knee cartilage: A study of proliferation, programmed cell death (apoptosis), and viability of chondrocytes in normal and osteoarthritic human knee cartilage." Arthritis & Rheumatism **44**(6): 1304-1312.
3. Allan, C.G., Hochberg, M.C., Mead, L.A., Wang, N.Y., Wigley, F.M., Klag, M.J. (2000). "Joint injury in young adults and risk for subsequent knee and hip osteoarthritis." Annals of Internal Medicine **133**: 321-328.
4. Arakoski, J.P.A., Jurvelin, J.S., Vaatainen, U., Helminen, H.J. (2000). "Normal and pathological adaptations of articular cartilage to joint loading." Scandinavian Journal of Medicine & Science in Sports **10**: 186-198.
5. Borelli Jr, J., Torzilli, P.A., Grigiene, R., Helfet, D.L. (1997). "Effect of impact load on articular cartilage: development of an intra-articular fracture model." Journal of Orthopaedic Trauma **11**(5): 319-326.
6. Brown, T. D. (2000). "Techniques for mechanical stimulation of cells in vitro: a review." Journal of Biomechanics **33**: 3-14.
7. Burns, K. (1999). Forensic Anthropology Training Manual. Upper Saddle River, NJ, Prentice-Hall, Inc.
8. Chen, C.T., Bhargava, M., Lin, P.M., Torzilli, P.A. (2003). Time, stress, and location dependent chondrocyte death and collagen damage in cyclically loaded articular cartilage. Journal of Orthopedic Research.
9. Chen, C.T., Burton-Wurster, N., Borden, C., Hueffer, K., Bloom, S.E., Lust, G. (2001). "Chondrocyte necrosis and apoptosis in impact damaged articular cartilage." Journal of Orthopaedic Research **19**(4): 703-711.
10. Choinski Jr, J. S. Home page. 12 May 2004.  
<<http://www.faculty.uca.edu/~johnc/proteoglycan.jpg>>
11. Clark, A.L., Barclay, L.D., Matyas, J.R., Herzog, W. (2003). "In situ chondrocyte deformation with physiological compression of the feline patellofemoral joint." Journal of Biomechanics **36**: 553-568.



12. Creamer, P. and M. C. Hochberg (1997). "Osteoarthritis." The Lancet **350**: 503-509.
13. D'Lima, D.D., Hashimoto, S., Chen, P.C., Colwell Jr, C.W., Lotz, M.K. (2001). "Human chondrocyte apoptosis in response to mechanical injury." Osteoarthritis and Cartilage **9**(8): 712-719
14. Duda, G.N., Eilers, M., Loh, L., Hoffman, J.E., Kaab, M., Schaser, K. (2001). "Chondrocyte death precedes structural damage in blunt impact trauma." Clinical Orthopaedics **393**: 302-309.
15. Eckstein, F., Lemberger, B., Stammberger, T., Englmeier, K.H., Reiser, M. (2000). "Patellar cartilage deformation in vivo after static versus dynamic loading." Journal of Biomechanics **33**: 819-825.
16. Edmondson, J.M., Armstrong, L.S., Martinez, A.O. (1988). "A rapid and simple MTT-based spectrophotometric assay for determining drug sensitivity in monolayer cultures." Journal of Tissue Culture Methods **11**(1): 15-17.
17. Ewers, B.J., Jayaraman, V.M., Banglmaier, R.F., Haut, R.C. (2002). "Rate of blunt impact loading affects changes in retropatellar cartilage and underlying bone in the rabbit patella." Journal of Biomechanics **35**: 747-755.
18. Ewers, B.J., Dvoracek-Driksna, D., Orth, M.W., Haut, R.C. (2001). "The extent of matrix damage and chondrocyte death in mechanically traumatized articular cartilage explants depends on rate of loading." Journal of Orthopaedic Research **19**(5): 779-784.
19. Frenkel, S. R. and P. E. Di Cesare (1999). "Degradation and repair of articular cartilage." Frontiers in Bioscience **4**: 671-685.
20. Fung, Y. C. (1993). Biomechanics. Mechanical Properties of Living Tissues, 2nd edition. New York, Springer-Verlag.
21. Guilak, F., Jones, W.R., Ting-Beall, P., Lee, G.M. (1999). "The deformation behavior and mechanical properties of chondrocytes in articular cartilage." Osteoarthritis and Cartilage **7**: 59-70.
22. Guilak, F., Meyer, B.C., Ratcliffe, A., Mow, V.C. (1994). "The effects of matrix compression on proteoglycan metabolism in articular cartilage explants." Osteoarthritis and Cartilage **2**(2): 91-101.
23. Hashimoto, S., Ochs, R.L., Komiya, S., Lotz, M.K. (1998). "Linkage of chondrocyte apoptosis and cartilage degeneration in human osteoarthritis." Arthritis & Rheumatism **41**(9): 1632-1638.

24. Hashimoto, S., Ochs, R.L., Rosen, F., Quach, J., McCabe, G., Solan, J., Seegmiller, J.E., Terkeltaub, R., Lotz, M.K. (1998). "Chondrocyte-derived apoptotic bodies and calcification of articular cartilage." Proceedings of the National Academy of Sciences **95**: 3094-3099.
25. Jeffrey, J.E., Gregory, D.W., Aspden, R.M. (1995). "Matrix damage and chondrocyte viability following a single impact load on articular cartilage." Archives of Biochemistry and Biophysics **322**(1): 87-96.
26. Johnston, S. A. (1997). "Osteoarthritis. Joint anatomy, physiology and pathobiology." Vet Clin North Am Small Anim Pract. **27**(4): 699-723.
27. Kiviranta, I., Jurvelin, J.S., Tammi, M., Saamanen, A.M., Helminen, H.J. (1985). "Microspectrophotometric quantitation of glycosaminoglycans in articular cartilage sections stained with Safranin O." Histochemistry **82**: 249-255.
28. Krueger, J.A., Thisse, P., Ewers, B.J., Dvoracek-Driksna, D., Orth, M.W., Haut, R.C. (2003). "The extent and distribution of cell death and matrix damage in impacted chondral explants varies with the presence of underlying bone." Journal of Biomechanical Engineering **125**(1): 114-119.
29. Kurz, B., Jin, M., Patwari, P., Cheng, D.M., Lark, M.W., Grodzinsky, A.J. (2001). "Biosynthetic response and mechanical properties of articular cartilage after injurious compression." Journal of Orthopaedic Research **19**: 1140-1146.
30. Lafeber, F.P., van der Kraan, P.M., van Roy, H.L., Vitters, E.L., Huber-Bruning, O., van den Berg, W.B., Bijlsma, J.W. (1992). "Local changes in proteoglycan synthesis during culture are different for normal and osteoarthritic cartilage." American Journal of Pathology **140**(6): 1421-1429.
31. Lewis, J.L., Deloria, L.B., Oyen-Tiesma, M., Thompson Jr, R.C., Ericson, M., Oegema Jr, T.R. (2003). "Cell death after cartilage impact occurs around matrix cracks." Journal of Orthopaedic Research **21**: 881-887.
32. Leddy, H. A. and F. Guilak (2003). "Site-specific molecular diffusion in articular cartilage measured using fluorescence recovery after photobleaching." Annals of Biomedical Engineering **31**: 753-760.
33. Lee, T. C., T. L. Arthur, et al. (2000). "Sequential labelling of microdamage in bone using chelating agents." The Journal of Bone and Joint Surgery **18**: 322-325.

34. Loening, A.M., James, I.E., Levenston, M.E., Badger, A.M., Frank, E.H., Kurz, B., Nuttall, M.E., Hung, H.H., Blake, S.M., Grodzinsky, A.J., Lark, M.W. (2000). "Injurious mechanical compression of bovine articular cartilage induces chondrocyte apoptosis." Archives of Biochemistry and Biophysics **381**(2): 205-212.
35. Lotz, M.K., Hashimoto, S., Kuhn, K. (1999). "Mechanisms of chondrocyte apoptosis." Osteoarthritis and Cartilage **7**: 389-391.
36. Lucchinetti, E., Adams, C.S., Horton Jr, W.E., Torzilli, P.A. (2002). "Cartilage viability after repetitive loading: a preliminary report." Osteoarthritis and Cartilage **10**(1): 71-81.
37. Majno, G. and I. Joris (1995). "Apoptosis, oncosis, and necrosis. An overview of cell death." American Journal of Pathology **146**(1): 3-13.
38. Medical Imagery. Carrico, P. and L. Shavell. 1994. 12 May 2004.  
<<http://www.MedImagery.net>>
39. Myers, R. E. and V. C. Mow (1983). Biomechanics of articular cartilage and its response to biomechanical stimuli. Cartilage: Structure, Function and Biochemistry. B. K. Hall. **1**.
40. Nordin, M. and V. H. Frankel (2001). Basic Biomechanics of the Musculoskeletal System. Baltimore, Lippincott, Williams & Wilkins.
41. Patwari, P., Gaschen, V., James, I.E., Berger, E., Blake, S.M., Lark, M.W., Grodzinsky, A.J., Hunziker, E.B. (2004). "Ultrastructural quantification of cell death after injurious compression of bovine calf articular cartilage." Osteoarthritis and Cartilage **12**: 245-252.
42. Patwari, P., Cook, M.N., DiMicco, M.A., Blake, S.M., James, I.E., Kumar, S., Cole, A.A., Lark, M.W., Grodzinsky, A.J. (2003). "Proteoglycan degradation after injurious compression of bovine and human articular cartilage in vitro." Arthritis & Rheumatism **48**(5): 1292-1301.
43. Poole, A. R. (1999). "An introduction to the pathophysiology of osteoarthritis." Frontiers in Bioscience **4**: 662-670.
44. Quinn, T.M., Morel, V., Meister, J.J. (2001). "Static compression of articular cartilage can reduce solute diffusivity and partitioning: implications for the chondrocyte biological response." Journal of Biomechanics **34**: 1463-1469.
45. Quinn, T.M., Allen, R.G., Schalet, B.J., Perumbuli, P., Hunziker, E.B. (2001). "Matrix and cell injury due to sub-impact loading of adult bovine articular

cartilage explants: effects of strain rate and peak stress.” Journal of Orthopaedic Research **19**: 242-249.

46. Ratcliffe, A. and V. C. Mow (1996). Articular Cartilage. Extracellular Matrix, Volume 1, Tissue Function. W. D. Comper. Amsterdam, Harwood Academic Publishers GmbH. **1**: 234-302.
47. Redman, S.N., Dowthwaite, G.P., Thomson, B.M., Archer, C.W. (2004). “The cellular responses of articular cartilage to sharp and blunt trauma.” Osteoarthritis and Cartilage **12**: 106-116.
48. Rowan, A. D. (2001). “Cartilage catabolism in arthritis: factors that influence homeostasis.” Expert Reviews in Molecular Medicine.
49. Royce, P. M. and B. S. Steinmann, eds. (1993). Connective Tissue and Its Heritable Disorders: Molecular, Genetic, and Medical Aspects. New York, NY, Wiley-Liss.
50. Sauerland, K., Raiss, R.X., Steinmeyer, J. (2003). “Proteoglycan metabolism and viability of articular cartilage explants as modulated by the frequency of intermittent loading.” Osteoarthritis and Cartilage **11**: 343-350.
51. Shimuzu, C., Coutts, R.D., Healey, R.M., Kubo, T., Hirasawa, Y., Amiel, D. (1997). “Method of histomorphometric assessment of glycosaminoglycans in articular cartilage.” Journal of Orthopaedic Research **15**: 670-674.
52. Shin, D., Lin, J.H., Agrawal, C.M., Athanasiou, K. (1997). Zonal variation in mechanical properties of articular cartilage. Biomedical Engineering Society Annual Fall Meeting.
53. Smith, R.L., Trindade, M.C.D., Ikenoue, T., Mohtai, P.D., Das, P., Carter, D.R., Goodman, S.B., Schurman, D.J. (2000). “Effects of shears stress on articular chondrocyte metabolism.” Biorheology **37**: 95-107.
54. Tew, Simon R., Kwan, Alvin P.L., Hann, A., Thomson, B.M., Archer, C.W. (2000). “The reactions of articular cartilage to experimental wounding.” Arthritis & Rheumatism **43**(1): 215-255.
55. Torzilli, P.A., Grigiene, R., Borelli Jr, J., Helfet, D.L. (1999). “Effect of impact load on articular cartilage: cell metabolism and viability, and matrix water content.” Journal of Biomechanical Engineering **121**: 433-440.
56. Triantafillopoulos, I.K., Papagelopoulos, P.J., Politi, P.K., Nikiforidis, P.A. (2002). “Articular changes in experimentally induced patellar trauma.” Knee Surg, Sports Traumatol, Arthrosc **10**: 144-153.

57. Virag, L., Kerekgyarto, C., Fachel, J. (1995). "A simple, rapid and sensitive fluorimetric assay for the measurement of cell-mediated cytotoxicity." Journal of Immunological Methods **185**: 199-208.
58. Wilson, W., van Rietbergen, B., van Donkelaar, C.C., Huijskes, R. (2003). "Pathways of load-induced cartilage damage causing cartilage degeneration in the knee after meniscectomy." Journal of Biomechanics **36**: 845-851.
59. Zhang, H., Vrahas, M.S., Baratta, R.V., Rosler, D.M. (1999). "Damage to rabbit femoral articular cartilage following direct impacts of uniform stresses: in vitro study." Clinical Biomechanics **14**: 543-548.

## APPENDICES

### A. Porcine Patella Removal

#### Materials:

Paired porcine knee joints (with joint capsule intact)  
Sterile table covers (Bio-shield Regular Sterilization Wrap, Allegiance # 4030)  
No.22 sterile surgical blades (Feather, cat# 72044-22)  
Single edged industrial razor blades (VWR Scientific, no.55411-005)  
400ml plastic beakers  
Sterile stainless steel large forceps  
Sterile stainless steel small forceps  
Sterile plastic squirt bottle (Nalgene, USA # 2405-0500)  
Protective eyewear  
Face mask  
Sterile and non-sterile latex surgical gloves  
Sterile cotton pads (VWR Scientific, cat# 21902-985)  
Sterile stainless steel bowl  
Sterile surgical gowns  
Dulbecco's Phosphate Buffered Saline (Sigma, no.D-8862, Lot 70K2343)  
Pennicilin with Streptomycin (Sigma, no. P-4333, Lot 100K2405)  
70% EtOH  
Betadine solution (The Purdue Frederick Co., CT, USA, Lot #4D91)

#### Procedure:

- 1) Lay down sterile table covers onto a clean countertop. Put on non-sterile gloves and protective eyewear.
- 2) Before proceeding, make sure that there are no holes in the synovial capsule of the leg.
- 3) Thoroughly spray fresh porcine leg with betadine and wipe down with a cotton pad.
- 4) Spray leg with 70% EtOH prior to cutting.
- 5) Transfer leg onto a fresh sterile table cover. Dispose non-sterile gloves and put on sterile gloves.
- 6) Using no.22 blade and tweezers, cut away tissue surrounding patella (careful not to puncture joint capsule).
- 7) With razor blade, gently carve away small tissue fibers that are closest to the bone (keeping patella attached to knee joint as long as possible).
- 8) Remove remaining connective tissue surrounding the outer edges of the cartilage surface of the patella using the razor blade. Gently cut along outer edge, careful not to injure the cartilage surface, until patella is completely detached from the joint.

- 9) Once removed from the joint, place the patella on saline soaked sterile cotton pads (which are kept in the steel bowl) and finish cleaning soft tissue off bony surface.
- 10) Spray patella with PBS using a sterile squirt bottle to wash away any surface bacteria or particles.
- 11) Keep patella soaked in a plastic beaker filled with PBS + antibiotics until ready for impaction.

## **B. *In vitro* Articular Cartilage Impaction**

### Materials:

Sterile razor blade  
Sterile porcine patellae  
MTS Mini-Bionix II hydraulic load frame (MTS Corp., Minneapolis MN, USA)  
Dulbecco's Phosphate Buffered Saline (Sigma, no.D-8862, Lot 70K2343)  
Spray bottle  
Stainless steel cylindrical impactor  
Wooden applicator sticks (Puritan, USA # 807)  
PMMA (Osteobond Copolymer Bone Cement, Zimmer Inc., USA #1101-08)  
Spherically bottomed mold  
X-Y positioning jig  
Green tissue marking dye (Polysciences, Inc. USA #24110)  
Sterile gloves

### Procedure:

- 1) Keep patellae moist throughout patellar impaction procedure by spraying them periodically with saline solution.
- 2) Press the bony non-articular surface into partially set PMMA, in a spherically bottomed mold to create an imprint. Remove patella immediately to prevent any heat related damage.
- 3) When PMMA is completely set, embed the patella in the cement.
- 4) Place specimen on x-y positioning jig. Rotate the patella and align the facets as needed.
- 5) Prior to impaction, mark patellae with tissue marking dye (to be used as reference markers) with the wooden applicator stick.
- 6) With hydraulic load frame (using the long axis of the cylinder) impact loading at a rate of 25 mm/sec to pre-selected force levels: 1000 N and 2000 N. Use a non-impacted level for a control.

### C. Patella Incubation: *in vitro* Organ Culture

Materials:

*For 10 bottles of culture:*

(10) 500 ml bottle Delbeco's MEM/Ham's F12 (Sigma, no.D8437, Lot 100K2316)

(1) 500 ml bottle of 10% Fetal Bovine Serum (Sigma, no.F-2442, Lot 110K8403)

(1) bottle of Penicillin with Streptomycin (Sigma, no.P4333, Lot 100K2405)

125mg Ascorbic acid (Sigma, no.F2442, Lot 50K0688)

50ml Distilled H<sub>2</sub>O

100x80mm Pyrex Dishes (Corning, no.3250-DO)

Fischer Scientific CO<sub>2</sub> Water-Jacketed Incubator

2 copper pennies (prevents fungus growth in incubator pan)

Rocking platform (VWR Scientific Products, Model 200)

Sterile dH<sub>2</sub>O

Laminar Flow hood

Sterile stainless steel large forceps

400ml plastic beakers

Sterile plastic squirt bottle (Nalgene, USA # 2405-0500)

Electric stirrer

Electronic scale

Sterile gloves

Sterile 5 ml pipettes

Sterile 10ml pipettes

Sterile 50 ml pipettes

Sterile 100ml pipettes

Pipet-aid

Sterile 60 ml syringe and needle

Sterile syringe filter

Sterile stainless steel patella stands

Plastic tube

Aspirating Pipette

Aspirating flask

Aspirator

Vacuum pump

Procedure:

*Preparation of 1 bottle of Media:*

1) Pipet 50ml of FBS into each of 10 bottles of MEM/Ham's F12 using a 50ml sterile pipette.

2) Transfer 5ml of Penn-Strep to each bottle of the MEM/Ham's F12 solution using a 10ml sterile pipette.

3) Weigh 125 mg Ascorbic acid and dissolve in 50ml of deionized water. Add 5ml of this solution to each bottle of MEM/F12 mixture using a sterile 60ml syringe with a sterile filter.



*Incubating the Patella:*

- 1) Separate each patella from the PMMA.
- 2) Using 3 plastic beakers, wash the first patella three times in PBS with antibiotics in beaker #1. Let patella soak in PBS for about 5 minutes before transferring it to the next beaker (#2 then #3). For the second patella, dispose of beaker #1 and use beaker #2 to replace it. Fill another beaker with fresh PBS and use it as beaker #3. Repeat for the 3<sup>rd</sup> patella. Irrigate the patella with PBS and antibiotics using a sterile squirt bottle.
- 3) Carefully (avoiding fingers from touching the rim) remove the lid of a Pyrex dish and place it rim side up on the counter. Place a patella holder inside the dish using a pair of sterile tongs.
- 4) Fill the dish with the media mixture, enough to completely immerse the patella.
- 5) Place the dish on the rocking shaker (speed=1.5) in the humidified incubator.
- 6) Keep the culture dish at 37°C in the incubator with 5% CO<sub>2</sub>.
- 7) Change the media daily. Do all steps under a fume hood, careful not to place hands (or other non-sterile objects) on or over the specimen and media.

*Changing the Media:*

- 1) After spraying gloves with EtOH, remove the dish from the incubator and place under the fume hood.
- 2) Attach a sterile 5ml aspirating pipette to the tube on the aspirator.
- 3) Remove the cover of the dish and place it rim side up on the counter.
- 4) Turn on the aspirator and hold the dish on an angle (to avoid putting hands over it).
- 5) Using the pipette attached to the aspirator, suck out all of the old media. If a significant amount of solid debris is present on the bottom of the dish, (if a significant amount of solid debris is present in the dish, wash patella once with PBS with antibiotics).
- 6) Quickly pour enough fresh media mixture to completely cover the patella.
- 7) Carefully put the cover back on the dish and place it in the incubator.
- 8) Change the media once daily for 3, 7 or 14 days, depending on each patella.

## **D. Histology**

### **D.1 Cell Viability Stain**

Materials:

Dulbecco's Modified Eagle's Medium:F-12 (Sigma no.D6434, Lot 22K2419)

MTT (Thiazolyl Blue, 98%) (Sigma no.M-5655, Lot 90K5317)

PBS (non-sterile)

Sample vials w/ lids

No.10 scalpel blade w/ handle (Electron Microscopy Sciences, PA, USA #72044-10)

400ml plastic beaker  
Table cover  
Electric band saw  
Yellow tissue marking dye (Polysciences, Inc. USA #24112)  
Wood applicator stick (Puritan, USA # 807)  
Stainless steel small forceps  
Protective eyewear  
Latex surgical gloves

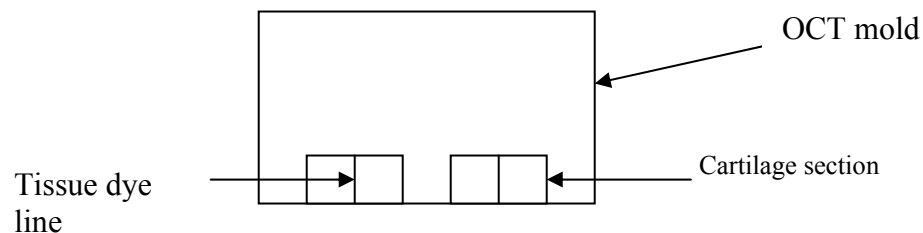
*Preparation of MTT stock solution (1 facet):*

1. Measure out 20 mg of MTT (Thiazoyl Blue) and dissolve in 4ml “Clear” DMEM Ham’s F-12, per facet.
2. Using a sterile filter and syringe, add the above mixture to an empty container.
3. When staining tissue, use 0.1ml of the above stock MTT per 1ml DMEM Ham’s F-12. (For example, use ~4ml of stock MTT per 36ml Ham’s F-12)

Procedure:

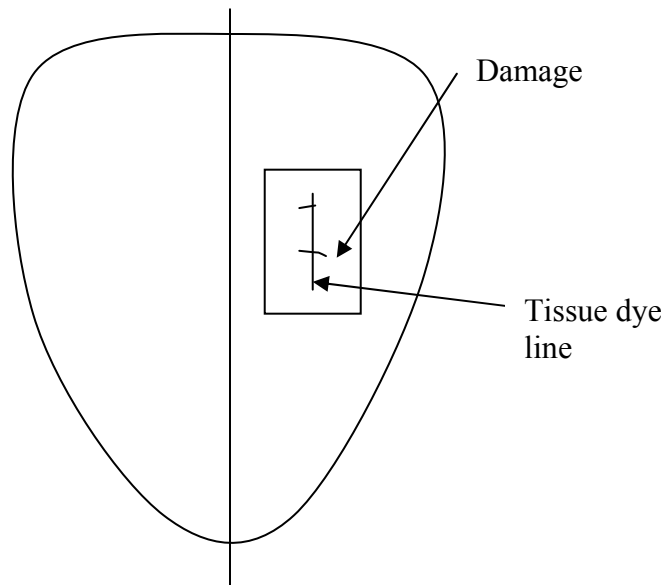
*Cutting Sections:*

1. Place table cover on counter and fill a 400ml plastic beaker with PBS (enough to use for rinsing the patella).
2. Using an autopsy saw, cut the cartilage+bone surface from the patella. Cut the specimen in half, separating the medial and lateral facets.
3. Make sure the line drawn between the two dots of tissue dye are visible. If not, re-apply the dye to the cartilage surface using a wooden applicator stick.
4. Place the medial facet in a beaker containing 0.1ml MTT solution per 1ml Ham’s F-12 in a 150ml beaker.
5. Let the sample sit overnight in the humidified incubator.
6. Cut a rectangular section of cartilage (see #3 below) from the lateral facet and freeze in OCT. See Tissue Freezing protocol.
7. Note any damage seen on either facet. If there is damage present, cut through the length of the “crack” and mount this section of tissue in OCT with the damaged edge up against the edge of the OCT mold. For example:



*Harvesting Sections:*

1. After 24hrs, remove the samples from the MTT solution and soak them 3X with PBS.
2. Put the samples in a vial filled with Formalin until ready to cut cartilage sections (see next step).
3. Using a scalpel, cut the cartilage off the bone in a rectangular shape, cutting around the tissue dye line. Make sure to include any damaged areas in the section (see #7). For example:



4. Put the section in a plastic vial containing 60% OCT with PBS for 24 hrs.
5. After 24 hrs, transfer the section to 80% OCT with PBS for 24 hrs.
6. After 24 hrs, transfer the section to 90% OCT with PBS until ready for freezing.

## **D.2 Tissue Freezing**

**Materials:**

Liquid nitrogen **OR** Dry Ice + 100% EtOH

Tissue-Tek O.C.T. Compound, Sakura Finetek (VWR Scientific Products, no.25608-930)

Tissue-Tek Cryomolds, Sakura Finetek (VWR Scientific Products, no. 4557)

Stainless steel small forceps

Stainless steel large forceps

Stainless steel container

Latex gloves

Protective eyewear

Aluminum foil

**Procedure:**

1. Pour the liquid nitrogen in the steel container (to about  $\frac{1}{2}$  inch high) **OR** if using dry ice, fill about  $\frac{1}{3}$  of the steel container with 100% EtOH and drop 5-6 pellets of dry ice into it. When the liquid ceases to fizz, it is cold enough for freezing.
2. Squeeze the OCT gel into the embedding container until it reaches the top of the container.
3. Cut the rectangular cartilage section in half, perpendicular to the tissue dye line.
4. Using the small forceps, place the two tissue halves side-by-side into the gel.
5. Using the large forceps, place the embedding container (with the gel and tissue specimen) in the liquid nitrogen or EtOH. Be careful not to let the nitrogen touch the OCT gel because it will cause it to boil.
6. When all of the gel turns white, quickly remove it from the liquid. Leaving the gel in too long will cause it to crack.
7. Pop the frozen block out of the embedding container and wrap it in aluminum foil. Keep the specimen in the freezer until ready for use.

Note: For best results, keep the OCT Embedding Gel in the refrigerator and the steel pan in the freezer until ready for use. This keeps the liquid nitrogen from spattering when coming in contact with room temperature objects.

## E. Cell Viability Data

Table 5. Data: Percentage of Dead Cells by Tissue Depth

D1 = Depth 1

		<b>D1</b>	<b>D2</b>	<b>D3</b>	<b>D4</b>	<b>D5</b>	<b>D6</b>	<b>D7</b>	<b>D8</b>	<b>D9</b>	<b>D10</b>
<b><u>All Specimens</u></b>											
<b>Observations (N)</b>	2390	244	244	244	242	240	238	235	233	235	235
<b>% Dead Mean</b>	15.7163	10.4708	3.12709	8.88418	12.7677	16.2222	16.958	19.2138	22.5014	21.8132	26.2684
<b>%Dead StdDev</b>	21.2922	16.5887	6.9735	14.5634	17.2067	19.5194	22.0141	23.7762	25.8917	23.0196	25.8165
<b><u>All: Controls</u></b>											
<b>Observations (N)</b>	793	80	80	80	80	79	80	79	78	78	79
<b>% Dead Mean</b>	6.40743	2.99137	0.80087	2.38475	4.64612	7.61595	6.17887	7.82063	8.4406	9.8396	13.61493
<b>%Dead StdDev</b>	12.7415	4.8483	2.5395	5.9289	9.03853	11.3827	14.0651	15.0494	14.8137	15.4862	18.8119
<b><u>All: Mediums</u></b>											
<b>Observations (N)</b>	807	82	82	82	82	81	80	79	79	80	80
<b>% Dead Mean</b>	19.5532	12.8778	4.7245	13.0113	17.5979	16.8829	20.3324	21.8802	27.8267	26.6562	34.6579
<b>%Dead StdDev</b>	21.2579	14.4829	7.7987	15.25703	19.1177	20.03624	21.5724	22.014	25.9534	22.0901	23.0106
<b><u>All: Highs</u></b>											
<b>Observations (N)</b>	790	82	82	82	80	80	78	77	76	77	76
<b>% Dead Mean</b>	21.1411	15.3607	3.7991	11.0979	15.9385	24.0517	24.5526	28.1673	31.3966	28.9106	30.5904
<b>%Dead StdDev</b>	24.8293	22.5289	8.3903	17.4727	18.5897	21.9457	24.9043	28.0572	28.8483	25.6607	29.8502

0 Days in Culture:

**C0**

<b>Observations (N)</b>	185	19	19	19	19	18	19	18	19	17	18
<b>% Dead Mean</b>	7.43286	0.421	0	1.3216	8.3958	12.8333	6.9695	11.9889	10.4095	8.5053	14.4922
<b>%Dead StdDev</b>	14.6126	1.8353	0	3.1444	13.3394	16.511	10.8286	15.6261	15.8992	13.1583	27.5817

**M0**

<b>Observations (N)</b>	193	20	20	20	20	20	19	18	18	19	19
<b>% Dead Mean</b>	18.7122	16.89	6.096	14.278	14.571	17.489	20.145	17.908	22.241	25.546	33.376
<b>%Dead StdDev</b>	24.714	21.89	10.072	19.887	22.103	26.051	25.877	24.754	31.454	26.083	29.579

**H0**

<b>Observations (N)</b>	199	21	21	21	20	20	20	19	19	19	19
<b>% Dead Mean</b>	19.4389	7.442	0.952	14.899	12.7005	21.7895	23.561	38.956	31.875	18.113	27.803
<b>%Dead StdDev</b>	25.2883	14.557	4.364	22.399	19.57	18.713	26.156	28.992	35.744	21.347	29.041

3 Days in Culture:

**C3**

<b>Observations (N)</b>	200	20	20	20	20	20	20	20	20	20	20
<b>% Dead Mean</b>	6.601	1.2935	0	4.2635	5.389	8.7225	7.2335	6.8035	10.2895	8.023	13.9925
<b>%Dead StdDev</b>	11.2909	4.3297	0	7.9624	7.2542	10.0363	12.0555	12.1401	16.3182	13.6327	13.889

**M3**

<b>Observations (N)</b>	194	20	20	20	20	19	19	19	19	19	19
<b>% Dead Mean</b>	23.2949	3.993	4.902	13.557	24.904	23.257	29.156	31.409	34.9	35.269	35.035
<b>%Dead StdDev</b>	22.7351	6.463	6.781	13.324	22.585	18.631	25.923	21.329	28.952	22.405	21.602

**H3**

<b>Observations (N)</b>	192	20	20	20	19	19	19	19	19	19	18
<b>% Dead Mean</b>	24.0981	16.201	5.834	15.179	20.636	20.911	25.199	29.919	31.728	40.868	37.032
<b>%Dead StdDev</b>	24.5778	21.318	10.47	21.075	21.526	21.09	27.194	27.203	23.871	22.118	28.822

7 Days in Culture:

**C7**

<b>Observations (N)</b>	210	21	21	21	21	21	21	21	21	21	21	21
<b>% Dead Mean</b>	5.9483	6.12048	1.54905	1.957619	2.0562	2.75	3.307	5.918	9.426	13.011	13.387	
<b>%Dead StdDev</b>	11.4937	5.27	3.507	5.21	4.824	4.707	6.365	14.153	16.0286	16.422	17.497	

**M7**

<b>Observations (N)</b>	210	21	21	21	21	21	21	21	21	21	21	21
<b>% Dead Mean</b>	20.739	13.198	3.432	16.174	17.975	15.337	19.806	27.109	32.383	24.463	37.511	
<b>%Dead StdDev</b>	18.9666	7.989	7.937	16.981	15.534	18.906	16.325	22.034	20.758	17.067	18.452	

**H7**

<b>Observations (N)</b>	199	21	21	21	21	21	19	19	18	19	19	19
<b>% Dead Mean</b>	19.118	29.133	3.735	3.069	15.982	21.983	27.112	25.307	17.969	23.507	25.603	
<b>%Dead StdDev</b>	26.2689	29.086	7.602	5.08	14.642	27.221	29.626	32.332	25.918	29.366	34.464	

14 Days in Culture:

**C14**

<b>Observations (N)</b>	198	20	20	20	20	20	20	20	18	20	20	
<b>% Dead Mean</b>	5.7407	3.845	1.577	1.9645	3.061	6.923	7.389	7.083	3.159	9.46	12.687	
<b>%Dead StdDev</b>	13.5134	5.033	3.361	6.291	8.323	10.497	22.605	18.192	9.346	18.44	15.971	

**M14**

<b>Observations (N)</b>	210	21	21	21	21	21	21	21	21	21	21	21
<b>% Dead Mean</b>	15.5913	17.197	4.541	8.123	13.145	12.085	13.045	11.434	21.659	22.061	32.622	
<b>%Dead StdDev</b>	17.6933	13.27	6.291	8.515	14.378	15.019	15.303	15.181	21.525	21.754	22.999	

**H14**

<b>Observations (N)</b>	200	20	20	20	20	20	20	20	20	20	20	20
<b>% Dead Mean</b>	22.0089	8.374	4.82	11.456	14.668	31.469	22.498	18.971	42.712	32.941	32.179	
<b>%Dead StdDev</b>	22.9229	16.268	9.757	14.043	18.827	19.316	16.879	21.082	25.058	24.817	27.84	

Table 6. Percentage of Dead Cells by Radial Position

	- 2r	- r	- r/2	center	r/2	r	2r
<b><u>All Specimens</u></b>							
<b>Observations (N)</b>	292	357	360	356	359	360	306
<b>% Dead Mean</b>	13.4508	15.4173	17.2218	17.2871	16.3116	16.894	12.6617
<b>%Dead StdDev</b>	19.9319	20.7118	22.1383	23.3172	21.3905	21.4209	19.0416
<b><u>All Controls</u></b>							
<b>Observations (N)</b>	88	119	120	117	120	120	109
<b>% Dead Mean</b>	2.90227	6.441	7.2572	6.01837	5.7938	8.3542	7.21486
<b>%Dead StdDev</b>	6.5521	12.2881	11.2738	12.49284	11.29663	16.22026	15.3774
<b><u>All Mediums</u></b>							
<b>Observations (N)</b>	110	119	120	120	119	120	99
<b>% Dead Mean</b>	16.4411	20.66	19.2043	21.0533	23.2788	19.9301	15.3501
<b>%Dead StdDev</b>	19.3478	23.2928	20.6955	22.4806	23.4839	19.5969	18.2414
<b><u>All Highs</u></b>							
<b>Observations (N)</b>	94	119	120	119	120	120	98
<b>% Dead Mean</b>	19.8269	19.151	25.2039	24.5684	19.621	22.3977	16.0042
<b>%Dead StdDev</b>	24.6409	21.8546	27.4739	27.907	23.0417	24.9752	22.1046



0 Days in Culture:

**C0**

<b>Observations (N)</b>	18	29	30	28	30	30	20
<b>% Dead Mean</b>	4.944	6.658	7.893	8.481	5.376	11.521	5.593
<b>%Dead StdDev</b>	11.0703	13.424	11.745	14.517	11.4499	22.679	12.333

**M0**

<b>Observations (N)</b>	30	29	30	30	29	30	15
<b>% Dead Mean</b>	19.02	19.369	17.221	20.815	22.9	17.387	10.159
<b>%Dead StdDev</b>	27.736	26.7799	22.263	27.773	27.461	19.326	17.5598

**H0**

<b>Observations (N)</b>	24	30	30	29	30	30	26
<b>% Dead Mean</b>	14.277	13.918	27.868	27.251	21.972	16.062	13.109
<b>%Dead StdDev</b>	25.969	18.385	33.341	30.869	22.619	20.035	18.846

3 Days in Culture:

**C3**

<b>Observations (N)</b>	20	30	30	30	30	30	30
<b>% Dead Mean</b>	2.783	8.867	7.576	4.677	7.482	9.277	4.273
<b>%Dead StdDev</b>	4.461	13.848	12.011	9.473	12.181	14.524	6.532

**M3**

<b>Observations (N)</b>	20	30	30	30	30	30	24
<b>% Dead Mean</b>	16.981	24.089	14.896	27.891	25.706	31.152	20.29
<b>%Dead StdDev</b>	14.1404	25.218	18.103	20.976	26.948	24.683	21.586

**H3**

<b>Observations (N)</b>	20	30	30	30	30	30	22
<b>% Dead Mean</b>	27.609	27.465	25.054	30.097	22.071	20.071	15.088
<b>%Dead StdDev</b>	23.564	19.344	24.102	29.652	26.555	22.208	24.677

7 Days in Culture

**C7**

<b>Observations (N)</b>	30	30	30	30	30	30	30
<b>% Dead Mean</b>	3.101	5.677	8.022	3.792	6.022	7.389	7.635
<b>%Dead StdDev</b>	5.809	12.69	12.948	7.121	13.153	12.794	13.394

**M7**

<b>Observations (N)</b>	30	30	30	30	30	30	30
<b>% Dead Mean</b>	18.253	22.267	25.628	21.096	23.235	21.222	13.472
<b>%Dead StdDev</b>	18.073	20.298	20.406	20.776	20.027	15.057	16.825

**H7**

<b>Observations (N)</b>	30	29	30	30	30	30	20
<b>% Dead Mean</b>	20.981	20.783	19.351	21.339	13.764	22.115	13.763
<b>%Dead StdDev</b>	27.218	26.914	28.537	28.641	21.115	27.006	24.431

14 Days in Culture:

**C14**

<b>Observations (N)</b>	20	30	30	29	30	30	29
<b>% Dead Mean</b>	0.884	4.5697	5.538	7.331	4.296	5.23	10.942
<b>%Dead StdDev</b>	2.748	8.788	8.214	16.817	8.104	12.973	23.519

**M14**

<b>Observations (N)</b>	30	30	30	30	30	30	30
<b>% Dead Mean</b>	11.6896	16.873	19.073	14.411	21.262	9.959	15.872
<b>%Dead StdDev</b>	12.0935	20.878	21.255	18.3499	19.447	11.174	16.879

**H14**

<b>Observations (N)</b>	20	30	30	30	30	30	30
<b>% Dead Mean</b>	16.973	14.492	28.543	19.676	20.678	31.342	20.679
<b>%Dead StdDev</b>	18.875	20.172	23.152	21.792	21.619	28.385	21.492

## F. Normalized Intensity Data: Proteoglycan Concentration

Table 7. Normalized Intensity by Tissue Depth  
D1 = Depth 1

		D1	D2	D3	D4	D5	D6	D7	D8	D9	D10
<b><u>All Specimens</u></b>											
<b>Norm Int N</b>	<b>Total</b>	239	238	237	238	236	236	234	234	234	232
<b>Norm Int Mean</b>	1.005	1.279	1.11	1.004	0.97	0.953	0.9405	0.936	0.921	0.919	1.011
<b>Norm Int StdDev</b>	0.236	0.218	0.249	0.232	0.22	0.216	0.215	0.228	0.205	0.174	0.123
<b><u>All Controls</u></b>											
<b>Norm Int N</b>	792	80	80	80	80	79	79	79	79	79	77
<b>Norm Int Mean</b>	1.003	1.33	1.18	1.06	0.982	0.922	0.892	0.878	0.867	0.884	1.034
<b>Norm Int StdDev</b>	0.241	0.23	0.238	0.239	0.22	0.191	0.184	0.174	0.156	0.13	0.134
<b><u>All Mediums</u></b>											
<b>Norm Int N</b>	800	82	81	80	81	80	80	79	79	79	79
<b>Norm Int Mean</b>	1.04	1.299	1.136	1.021	1.002	1.008	1	0.9931	0.974	0.961	1
<b>Norm Int StdDev</b>	0.193	0.218	0.239	0.172	0.156	0.158	0.162	0.156	0.144	0.125	0.085
<b><u>All Highs</u></b>											
<b>Norm Int N</b>	766	77	77	77	77	77	77	76	76	76	76
<b>Norm Int Mean</b>	0.9696	1.206	1.009	0.932	0.9244	0.925	0.928	0.936	0.922	0.913	0.998
<b>Norm Int StdDev</b>	0.265	0.188	0.241	0.261	0.269	0.275	0.274	0.312	0.28	0.238	0.142

*0 Days in Culture:*

**C0**

<b>Norm Int N</b>	209	21	21	21	21	21	21	21	21	21	20
<b>Norm Int Mean</b>	0.898	1.155	1.001	0.887	0.844	0.824	0.815	0.8121	0.801	0.839	1.004
<b>Norm Int StdDev</b>	0.179	0.261	0.201	0.12	0.108	0.108	0.111	0.107	0.095	0.106	0.121

**M0**

<b>Norm Int N</b>	180	20	19	18	19	18	18	17	17	17	17
<b>Norm Int Mean</b>	1.005	1.236	1.028	0.948	0.94	0.97	0.984	0.982	0.956	0.962	1.015
<b>Norm Int StdDev</b>	0.194	0.184	0.168	0.178	0.188	0.198	0.194	0.196	0.18	0.179	0.097

**H0**

<b>Norm Int N</b>	200	20	20	20	20	20	20	20	20	20	20
<b>Norm Int Mean</b>	1.168	1.346	1.19	1.151	1.147	1.145	1.144	1.194	1.164	1.1	1.096
<b>Norm Int StdDev</b>	0.342	0.236	0.342	0.355	0.356	0.359	0.361	0.44	0.375	0.353	0.194

*3 Days in Culture:*

**C3**

<b>Norm Int N</b>	200	20	20	20	20	20	20	20	20	20	20
<b>Norm Int Mean</b>	1.031	1.374	1.162	1.015	0.974	0.96	0.965	0.962	0.951	0.922	1.024
<b>Norm Int StdDev</b>	0.262	0.235	0.258	0.238	0.24	0.246	0.256	0.247	0.221	0.179	0.196

**M3**

<b>Norm Int N</b>	200	20	20	20	20	20	20	20	20	20	20
<b>Norm Int Mean</b>	0.952	1.191	0.979	0.899	0.9	0.91	0.895	0.908	0.921	0.925	0.994
<b>Norm Int StdDev</b>	0.132	0.098	0.094	0.076	0.098	0.108	0.109	0.115	0.118	0.097	0.106

**H3**

<b>Norm Int N</b>	170	17	17	17	17	17	17	17	17	17	17
<b>Norm Int Mean</b>	0.906	1.156	0.901	0.826	0.845	0.87	0.875	0.876	0.867	0.866	0.978
<b>Norm Int StdDev</b>	0.174	0.128	0.091	0.112	0.159	0.176	0.182	0.188	0.187	0.145	0.119

7 Days in Culture:

**C7**

<b>Norm Int N</b>	209	21	21	21	21	21	21	21	21	21	20
<b>Norm Int Mean</b>	1.003	1.349	1.2	1.085	1.001	0.926	0.872	0.853	0.839	0.862	1.042
<b>Norm Int StdDev</b>	0.226	0.158	0.163	0.206	0.208	0.182	0.171	0.151	0.126	0.106	0.097

**M7**

<b>Norm Int N</b>	210	21	21	21	21	21	21	21	21	21	21
<b>Norm Int Mean</b>	1.16	1.513	1.405	1.195	1.119	1.11	1.091	1.075	1.053	1.03	1.005
<b>Norm Int StdDev</b>	0.218	0.254	0.192	0.115	0.119	0.137	0.16	0.15	0.139	0.118	0.052

**H7**

<b>Norm Int N</b>	200	20	20	20	20	20	20	20	20	20	20
<b>Norm Int Mean</b>	0.916	1.102	0.969	0.897	0.888	0.891	0.892	0.882	0.867	0.844	0.926
<b>Norm Int StdDev</b>	0.138	0.093	0.129	0.132	0.124	0.128	0.134	0.137	0.131	0.113	0.083

14 Days in Culture:

**C14**

<b>Norm Int N</b>	174	18	18	18	18	17	17	17	17	17	17
<b>Norm Int Mean</b>	1.098	1.454	1.385	1.269	1.131	0.995	0.928	0.893	0.883	0.922	1.073
<b>Norm Int StdDev</b>	0.252	0.128	0.156	0.218	0.223	0.177	0.139	0.13	0.12	0.095	0.091

**M14**

<b>Norm Int N</b>	210	21	21	21	21	21	21	21	21	21	21
<b>Norm Int Mean</b>	1.035	1.246	1.113	1.027	1.039	1.033	1.023	1.001	0.958	0.924	0.991
<b>Norm Int StdDev</b>	0.151	0.142	0.213	0.141	0.109	0.114	0.121	0.121	0.111	0.072	0.083

**H14**

<b>Norm Int N</b>	196	20	20	20	20	20	20	19	19	19	19
<b>Norm Int Mean</b>	0.877	1.212	0.961	0.838	0.806	0.787	0.793	0.775	0.777	0.83	0.989
<b>Norm Int StdDev</b>	0.233	0.169	0.209	0.218	0.227	0.236	0.228	0.205	0.186	0.135	0.084

Table 8. Normalized Intensity by Radial Position

	<b>- 2r</b>	<b>- r</b>	<b>-r/2</b>	<b>center</b>	<b>r/2</b>	<b>r</b>	<b>2r</b>
<b><u>All Specimens</u></b>							
<b>Norm Int N</b>	319	356	360	360	354	352	257
<b>Norm Int Mean</b>	1.053	0.99	0.994	0.997	0.997	0.992	1.02
<b>Norm Int StdDev</b>	0.239	0.247	0.265	0.205	0.211	0.199	0.211
<b><u>All Controls</u></b>							
<b>Norm Int N</b>	99	120	120	120	120	120	93
<b>Norm Int Mean</b>	1.077	0.984	0.969	0.988	0.995	0.998	1.029
<b>Norm Int StdDev</b>	0.281	0.255	0.236	0.227	0.228	0.219	0.234
<b><u>All Mediums</u></b>							
<b>Norm Int N</b>	120	120	120	120	114	112	94
<b>Norm Int Mean</b>	1.032	1.019	1.035	1.047	1.052	1.038	1.066
<b>Norm Int StdDev</b>	0.204	0.202	0.194	0.188	0.187	0.178	0.196
<b><u>All Highs</u></b>							
<b>Norm Int N</b>	100	116	120	120	120	120	70
<b>Norm Int Mean</b>	1.056	0.966	0.978	0.957	0.946	0.943	0.946
<b>Norm Int StdDev</b>	0.384	0.279	0.34	0.188	0.202	0.184	0.18

*0 Days in Culture:*

**C0**

<b>Norm Int N</b>	29	30	30	30	30	30	30
<b>Norm Int Mean</b>	1.017	0.825	0.829	0.875	0.85	0.885	1.008
<b>Norm Int StdDev</b>	0.275	0.122	0.136	0.155	0.141	0.137	0.144

**M0**

<b>Norm Int N</b>	30	30	30	30	24	22	14
<b>Norm Int Mean</b>	1.004	0.949	1.004	0.983	1.037	1.04	1.067
<b>Norm Int StdDev</b>	0.227	0.208	0.186	0.18	0.176	0.165	0.21

**H0**

<b>Norm Int N</b>	30	30	30	30	30	30	20
<b>Norm Int Mean</b>	1.395	1.253	1.293	1.077	1.073	0.998	1.043
<b>Norm Int StdDev</b>	0.48	0.326	0.505	0.15	0.171	0.119	0.139

*3 Days in Culture:*

**C3**

<b>Norm Int N</b>	30	30	30	30	30	30	20
<b>Norm Int Mean</b>	1.087	1.035	0.994	1.032	1.028	1.016	1.021
<b>Norm Int StdDev</b>	0.36	0.311	0.224	0.225	0.229	0.197	0.273

**M3**

<b>Norm Int N</b>	30	30	30	30	30	30	20
<b>Norm Int Mean</b>	0.96	0.952	0.954	0.984	0.957	0.925	0.925
<b>Norm Int StdDev</b>	0.173	0.103	0.123	0.12	0.122	0.119	0.167

**H3**

<b>Norm Int N</b>	20	30	30	30	30	30	.
<b>Norm Int Mean</b>	0.882	0.84	0.868	0.932	0.933	0.972	.
<b>Norm Int StdDev</b>	0.207	0.183	0.142	0.148	0.179	0.171	.

7 Days in Culture:

**C7**

<b>Norm Int N</b>	30	30	30	30	30	30	29
<b>Norm Int Mean</b>	1.064	0.98	0.972	0.988	1.007	0.988	1.021
<b>Norm Int StdDev</b>	0.211	0.22	0.225	0.222	0.217	0.239	0.253

**M7**

<b>Norm Int N</b>	30	30	30	30	30	30	30
<b>Norm Int Mean</b>	1.126	1.166	1.187	1.168	1.167	1.129	1.173
<b>Norm Int StdDev</b>	0.205	0.215	0.226	0.249	0.234	0.205	0.2063

**H7**

<b>Norm Int N</b>	30	30	30	30	30	30	20
<b>Norm Int Mean</b>	0.886	0.888	0.89	0.939	0.92	0.948	0.95
<b>Norm Int StdDev</b>	0.183	0.102	0.147	0.114	0.136	0.119	0.149

14 Days in Culture:

**C14**

<b>Norm Int N</b>	10	30	30	30	30	30	14
<b>Norm Int Mean</b>	1.26	1.098	1.081	1.058	1.097	1.102	1.103
<b>Norm Int StdDev</b>	0.103	0.254	0.274	0.26	0.245	0.239	0.294

**M14**

<b>Norm Int N</b>	30	30	30	30	30	30	30
<b>Norm Int Mean</b>	1.037	1.007	0.995	1.052	1.045	1.059	1.053
<b>Norm Int StdDev</b>	0.181	0.189	0.146	0.114	0.134	0.154	0.13

**H14**

<b>Norm Int N</b>	20	26	30	30	30	30	30
<b>Norm Int Mean</b>	0.975	0.868	0.863	0.879	0.856	0.855	0.878
<b>Norm Int StdDev</b>	0.239	0.22	0.206	0.255	0.25	0.264	0.197